Chapter1
Introduction

In recent years, wireless communication has made our life convenient. With the progress of communication technologies, transmission data rate is increasing significantly such that audio and video data can be supported in the wireless communication. Orthogonal Frequency Division Multiplexing (OFDM) system is a promising system to support high data rate transmission and adopted in many recent wireless transmission standards, such as European Digital Audio Broadcasting (DAB), Digital Video Broadcasting Terrestrial (DVB-T), IEEE 802.11g standard for wireless LAN (Local Area Network), and IEEE 802.16a standard for wireless MAN (Metropolitan Area Network).

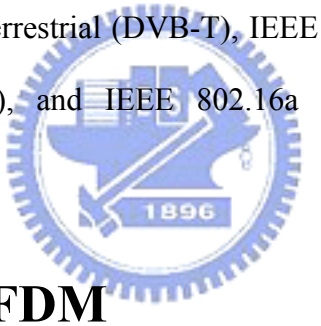

1.1 History of OFDM

The concept of Orthogonal Frequency Division Multiplexing (OFDM) has been known since 1966 [1]. Wideband signals are transmitted through multiple narrow band channels. In 1971, discrete Fourier transform (DFT) in the baseband modulation and demodulation was proposed to be used in OFDM systems [2].Without requirement of multiple oscillators to modulate different signals at different carriers, DFT-based OFDM was a crucial evolution because it made OFDM system implementation practical. In OFDM systems, symbol duration in each narrow band channel is increased thus inter-symbol interference (ISI) effect can be avoided. With the adding of cyclic prefix (CP), ISI and inter-carrier interference (ICI) problems can be solved at the same time [3]. Therefore, the channel effect can be compensated by

simple one tap equalizer. However, due to the sensitivity to frequency orthogonality, synchronization and channel estimation become critical issues in OFDM system.

1.2 Paper Surveys on OFDM Channel Estimators

In the literature, channel estimation methods can be basically classified as pilot-aided (PA) methods, decision directed (DD) and blind channel estimation methods. In the context of pilot-aided channel estimators, a subset of subcarriers are used to transmit known signals, called pilot signals, for sampling the desired channel response. The channels of unknown subcarriers are interpolated by pilot tones. In such a scenario, good bit error rate performance is achieved at the cost of a reduction of the number of useful subcarriers available for data transmission. The family of pilot-aided channel estimation techniques was investigated for example by [14] and [15]. In [14], piecewise-constant and piecewise-linear interpolations between pilots was proposed. In [15], channel estimation is performed by two dimension interpolation between pilots. In general, the pilot spacing must be denser than the coherent bandwidth to exploit correlations by interpolation. By contrast, in decision directed scenarios, the previous decision data and re-modulated subcarrier data symbols are considered as virtual pilot signals to estimate new channel responses. The family of decision directed channel estimation techniques was investigated for example by [16]. In [16], an MMSE-based frequency domain channel predictor was proposed for decision directed channel estimators. In such scenarios, the performance depends on the variation speed of the channels. If the successive channels are almost static, DD channel estimator will have good performance. Combined PA and DD channel estimators are investigated for example by [18], in such scenarios, both data decision

data and pilot signals are used to estimate channel response. Blind and semi-blind channel estimation methods for OFDM are proposed for example by [19]. Most of these methods are subspace-based approaches. Blind channel estimation achieves high bandwidth efficiency but usually need to use many OFDM blocks in order to obtain a good statistical estimate. Therefore, the performances of the blind channel estimation generally degrade in fast fading channels. In general downlink OFDM scenarios, the initial channel response can be estimated with preambles, which are usually an all-carriers known signal at the receiver end.

1.3 Motivation of This Thesis

In practical systems, guard bands are necessary to avoid interfering other systems. But preambles with guard bands are less discussed in the literature. In semi-blind channel estimation techniques, the accuracy of the initial channel estimation is very important. Generally, channel parameters in the time domain are less than that in the frequency domain. Therefore, channel tracking in the time domain is a reasonable method. However, to obtain channel impulse responses but no information in guard bands has some problems and the accuracy of estimated channel impulse responses becomes a crucial issue.

In this document, an initial channel estimation algorithm using preambles with guard bands, defined in IEEE 802.16 standard, followed by time domain paths tracking will be proposed (tracking methods are proposed by my senior classmate Meng-Ling Ku).

1.4 Organization of This Thesis

The organization of this thesis is as the following. In chapter 2, DFT-based OFDM systems and the characteristic of wireless multipath Rayleigh fading channels are introduced. Besides, several conventional channel estimators on OFDM systems are presented. In chapter 3, at first, an initial channel estimator based on multipath interference cancellation is proposed. Secondly, a Newton method is proposed to track the following OFDM symbols. Computer simulation results along with some discussions are showed in chapter 4. Finally, in chapter 5, brief conclusions are made.

Chapter2

Introduction of DFT-based OFDM Systems and Related Conventional Channel Estimation Techniques

The concept of Orthogonal Frequency Division Multiplexing (OFDM) is initiated from that of multi-carriers systems [2] [4]. Data are transmitted through multiple carriers simultaneously to achieve high data rate transmission. In order to do coherent detection accurately, channel estimation becomes a significant issue. In this chapter, DFT-based OFDM system and several conventional channel estimation methods will be introduced.

2.1 DFT-based OFDM System

DFT-based OFDM system will be introduced in this section.

2.1.1 OFDM modulator

If the discrete-time signal by sampling s(t) with sampling period $T_d = \frac{T}{N}$ is considered, s(t) can be synthesized as

$$s[n] = s(t)\Big|_{t=nT_d} = \frac{1}{N}\sum_{k=-\frac{N}{2}}^{\frac{N}{2}-1} X_k e^{j2\pi\frac{kn}{N}}, 0 \le \text{n} \le \text{N-1} = IDFT\{X_k\} \qquad (2.1)$$

where *IDFT* means Inverse Discrete Fourier Transform, N is the length of IDFT, T is the duration of one OFDM symbol, $X_k, k = 0 \cdots N-1$ are N input signals and $s[n], n = 0 \cdots N\text{-}1$, are N output sub-symbols of this OFDM modulation. A baseband OFDM modulator is illustrated as Fig. 2.1.

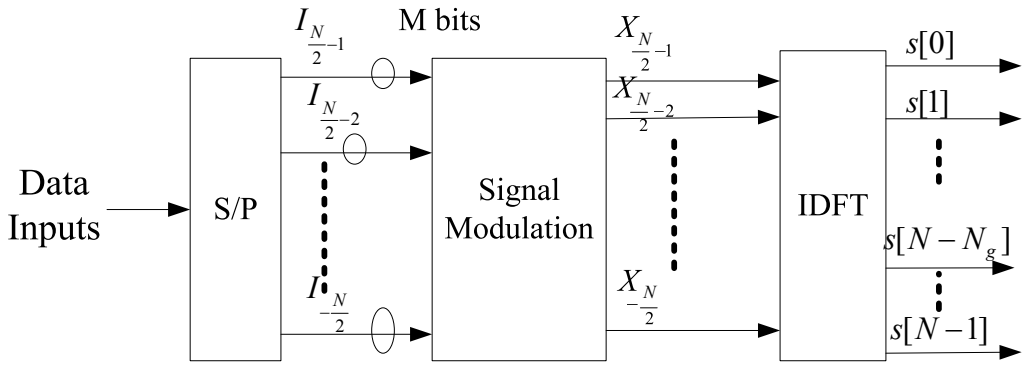

Figure 2.1 OFDM modulator

2.1.2 Cyclic Prefix (CP)

In multipath channels, delayed replicas of the previous OFDM signals lead to inter-symbol interference (ISI) between successive OFDM signals as showed in Fig. 2.2. If only a silent guard period is inserted between successive OFDM signals, intercarrier interference (ICI) will be induced because loss of orthogonality between subcarriers. In order to combat ISI and ICI problems at the same time, a copy of the last part of OFDM signals is attached to the front of itself [3]. Therefore, a complete OFDM symbol will be as Fig. 2.3 and bandwidth efficiency is decreased due to the CP. If the maximal channel delay spread is less than the length of CP, ISI problems can be solved. In current systems, one-fourth of the information signal length is an often candidate for CP length. A digital implementation with cyclic prefix extension OFDM transmitter is illustrated as Fig. 2.4.

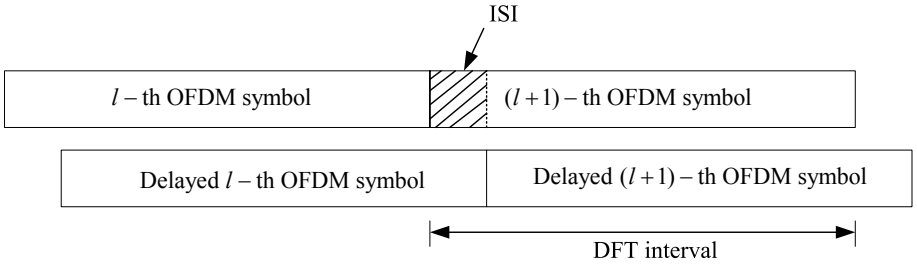

Figure 2.2 Concept of inter-symbol interference (ISI)

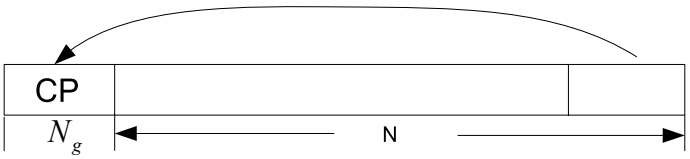

Figure 2.3: Complete OFDM symbol

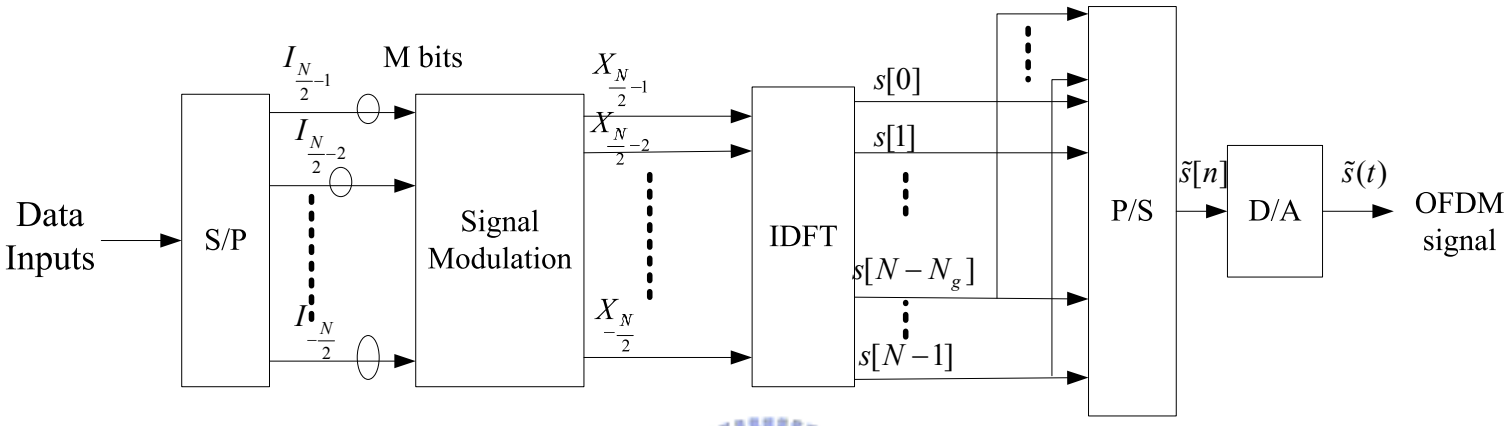

Figure 2.4 Cyclic prefix extension OFDM system transmitter

Therefore, complete OFDM signals can be described as

$$\tilde{s}[n] = \frac{1}{N} \sum_{k=-\frac{N}{2}}^{\frac{N}{2}-1} X_k e^{j2\pi \frac{k(n-N_g)_N}{N}} \qquad 0 \le \mathrm{n} \le \mathrm{N}+\mathrm{N_g}-1 \tag{2.2}$$

where N_g is the length of CP and $(n-N_g)_N$ means $(n-N_g)$ modulo N.

2.1.3 OFDM Demodulator

Received complete OFDM signals can be represented as

$$\tilde{r}[n] = \tilde{s}[n] * h[n] + z[n] \quad 0 \le n \le N + N_g + L_h - 2 \tag{2.3}$$

where $z[n]$ is AWGN and $h[n]$ is the channel responses with length L_h and notation $*$ means linear convolution.

Assume the multipath delay is less than the length of CP (L_h is less than $\mathrm{N_g}$), then

received useful part $r[n]$ (CP removed) can be represented as

$$r[n] = s[n] \otimes_N h[n] + z[n] \tag{2.4}$$

where notation $\otimes_N$ means N-point circular convolution.

Therefore, the received signals at the k-th subcarrier can be expressed as eq. (2.5), the structure of the OFDM system receiver is illustrated as Fig. 2.5. By eq. (2.5), the relationship between transmit signals and received signals can be equivalent to parallel Gaussian channels as shown in Fig. 2.6, and the channel effects can be compensated by a simple one-tap equalizer as shown in eq. (2.6)

$$\begin{aligned} Y_k &= FFT(r[n]) = FFT(s[n] \otimes_N h[n] + z[n]) \\ &= X_k H_k + Z_k \end{aligned} \tag{2.5}$$

Where H_k is the channel frequency responses of the k-th subcarrier and Z_k is AWGN of the k-th subcarrier in the frequency domain

$$\frac{Y_k}{H_k} = \frac{(X_k H_k + Z_k)}{H_k} = X_k + \frac{Z_k}{H_k} \tag{2.6}$$

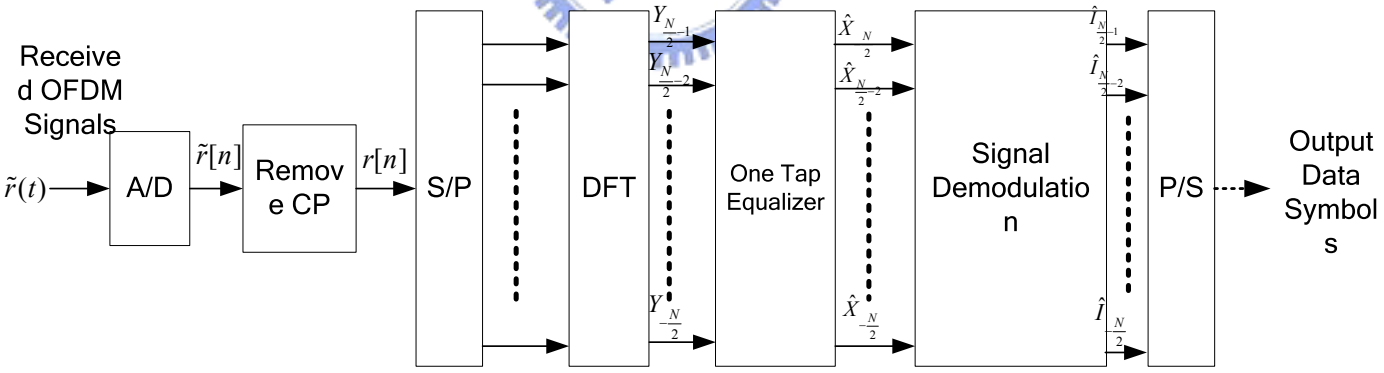

Figure 2.5: OFDM system receiver

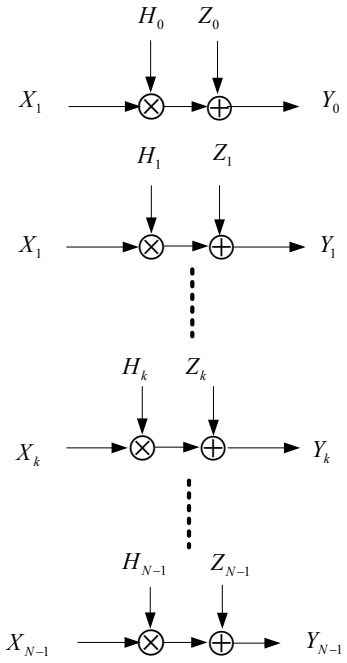

Figure 2.6 Equivalent channel model of OFDM systems

2.1.4 Advantages and Disadvantages of OFDM Systems

Advantages and disadvantages of OFDM systems are listed in the following.

- Advantages:

  (1) High transmission rate is supported.

  (2) Only a simple one-tap equalizer is needed due to flat fading per subcarrier.

  (3) Inter-symbol interference problems are alleviated.

- Disadvantages:

  (1) Due to demand for orthogonality between each subcarrier, OFDM systems are sensitive to synchronization.

  (2) The Peak to Average Power Ratio (PAPR) problem induces non-linear distortion.

2.2 Characteristics of Multipath Fading Channels

In wireless communications, received signals usually come from multiple paths due to reflection effects. Such environment is called a multipath channel. The equivalent baseband of a multipath channel impulse response can be described as [5]

$$h(t,\tau) = \sum_{l=0}^{l=L-1} a_l(t)\delta(t-\tau_l) \tag{2.7}$$

Where $a_l(t)$ and τ_l are the time-varying complex fading gain and the path delay of the l-th path, L is the total number of multipath, and δ is a delta function. In general, $a_l(t)$ are modeled as complex Gaussian process and different paths are uncorrelated (uncorrelated scattering), which is also known as a multipath Rayleigh fading channel. The variation speed of path gain $a_l(t)$ depends on maximal Doppler frequency or Doppler spread, which is proportioned to the vehicle speed and carrier frequency. Maximal Doppler frequency is defined as eq. (2.8).The larger the Doppler spread is, the faster variation of the path gains are. [6]

$$f_d = \frac{f_c v}{c} \tag{2.8}$$

where f_c is the central frequency and v is the vehicle speed and c is the speed of light. Generally, the coherence time of the channel can be approximated to the inverse of the Doppler spread. Therefore, the time variation speed of the channel is proportional to the inverse of the Doppler spread. On the other hand, in order to measure the variation in the frequency domain, multipath intensity profile or delay power spectrum for uncorrelated scattering channels is defined as

$$\varphi(\tau) = \frac{1}{2}\sum_l E[\|\alpha_l(t)\|^2 \delta(t-\tau_l)] \tag{2.9}$$

The range of τ over which $\varphi(\tau)$ is essentially nonzero is called the multipath

spread of the channel. The coherence bandwidth of the channel can be approximated to the inverse of the delay spread. Therefore, channel variation in the frequency domain is proportional to the inverse of the delay spread.

The equivalent time-varying channel frequency responses are described as

$$H(t,f)=\int_{-\infty}^{\infty}h(t,\tau)e^{-j2\pi ft}d\tau=\int_{-\infty}^{\infty}\sum_{l=0}^{l=L-1}a_l(t)\delta(t-\tau_l)e^{-j2\pi ft}d\tau$$
$$=\sum_{l=0}^{l=L-1}a_l(t)e^{-j2\pi f\tau_l} \tag{2.10}$$

In IFFT/FFT based OFDM systems, let eq. (2.10) $f=\frac{k}{T},k=0,\cdots,N-1$ and only sampling time $t=\frac{nT}{N},n=0,\cdots,N-1$ are considered, then the time varying discrete frequency responses can be described as

$$H(t,k)=\sum_{l=0}^{l=L-1}a_l(t)e^{\frac{-j2\pi k\tau_l}{N}} \tag{2.11}$$

where N is the length of Discrete Fourier Transform.

In the computer simulation, channel gains $a_l(t)$ are generated by Jakes model [7], the introduction of Jakes model is as following:

In the multipah Rayleigh fading channel without line of sight (LOS),the angel of the arrival signal in a plane is assumed to be uniformly distributed in the interval $[0,2\pi)$,as showed in Fig. 2.7.Jakes modeled the Rayleigh fading channel by a bank of oscillators with the maximal Doppler frequency and its fractions, as eq. (2.12) showed.

$$f_I(t)=2\sum_{n=1}^{N_0}\cos\beta_n\cdot\cos\omega_n t+\sqrt{2}\cos\alpha\cdot\cos\omega_d t$$
$$f_Q(t)=2\sum_{n=1}^{N_0}\sin\beta_n\cdot\cos\omega_n t+\sqrt{2}\sin\alpha\cdot\cos\omega_d t \tag{2.12}$$

where

$N = 2(2N_0 + 1), N_0 \geq 8$

$\omega_n = \omega_d \cos\alpha_n$ = Doppler shifts, $n = 1, 2, \cdots, N_0$

$\alpha_n = \frac{2\pi n}{N}$ = the arrival angel of the n-th arrival siganl, $n = 1, 2, \cdots, N_0$

β_n = the phase of the n-th arrival signal, $n = 1, 2, \cdots, N_0$

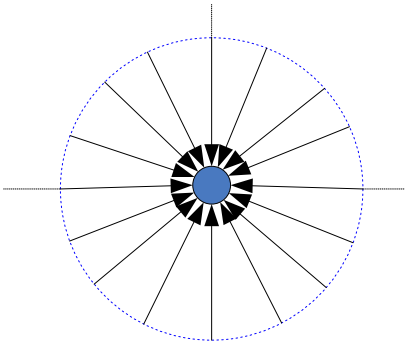

Figure 2.7 The multipath propagation model of Rayleigh fading channel

In eq. (2.12), N_0 must be large enough to approximate to the central theorem. β_n are chosen properly such that the arrival phases are close to uniform distribution in $[0, 2\pi)$.

2.3 Some Conventional Channel Estimators on OFDM Systems

Assume the multipath spread is less than the length of cyclic prefix, OFDM systems can be modeled as parallel Gaussian channels as shown in Fig. 2.6. Based on this model, channel effects can be compensated simply by a one tap equalizer. In order to coherent detect data accurately, correct channel estimation is important. In the following sections, several conventional channel estimators on OFDM systems will be introduced. Notation used is identical to that used in Fig. 2.6.

2.3.1 Least Square (LS) Channel Estimator

Least square channel estimator is the easiest estimator and common used in simple OFDM systems. The criterion of LS is defined as

$$\hat{H}_{kLS} = \arg\min_{H_k}\{(Y_k - H_k X_k)^2\} \tag{2.13}$$

where k is sub-carrier index and the notation min means minimization.

By (2.13), the LS channel estimator is to minimize square errors between received signals and attenuated transmitted signals in the frequency domain for every individual subcarrier. Differentiate $(Y_k - H_k X_k)^2$ with respect to H_k and let the results be zero, LS criterion can be solved as

$$\hat{H}_{kLS} = \frac{Y_k}{X_k} = \frac{X_k H_k + Z_k}{X_k} = H_k + \frac{Z_k}{X_k} = H_k + \tilde{Z}_k \tag{2.14}$$

where $\tilde{Z}_k = \frac{Z_k}{X_k}$.

This is to divide received signals by pre-known transmitted data at the receiver end.

Therefore, least square channel estimation can be described as

$$\hat{\mathbf{H}}_{\mathrm{LS}} = \begin{bmatrix} X_0 & 0 & \cdots & 0 \\ 0 & X_1 & & \vdots \\ \vdots & & \ddots & 0 \\ 0 & \cdots & 0 & X_{M-1} \end{bmatrix}^{-1} \begin{bmatrix} Y_0 \\ Y_1 \\ \vdots \\ Y_{M-1} \end{bmatrix} = \mathbf{X}^{-1}\mathbf{Y} = \begin{bmatrix} \frac{Y_0}{X_0} & \frac{Y_1}{X_1} \cdots \frac{Y_{M-1}}{X_{M-1}} \end{bmatrix}^T \tag{2.15}$$

where M means the number of pre-known transmitted data at the receiver end. $\mathbf{X} = \begin{bmatrix} X_0 & 0 & \cdots & 0 \\ 0 & X_1 & & \vdots \\ \vdots & & \ddots & 0 \\ 0 & \cdots & 0 & X_{M-1} \end{bmatrix}$, $\mathbf{Y} = \begin{bmatrix} Y_0 \\ Y_1 \\ \vdots \\ Y_{M-1} \end{bmatrix}$, and $\mathbf{X}^{-1}$ is the inverse of $\mathbf{X}$.

2.3.2 Linear Minimal Mean Square Error (MMSE) Channel Estimator [8]

Linear minimal mean square error channel estimators can be used to interpolate complete channel responses based on the LS solution of spare pilot tones or just refine the LS solutions of all-band pilot tones. The criterion of MMSE can be described as

$$\mathbf{H}_{\mathbf{MMSE}} = \arg\min_{\mathbf{W}\hat{\mathbf{H}}_{LS}} \{E[\mathbf{H} - \mathbf{W}\hat{\mathbf{H}}_{LS}]\} \tag{2.16}$$

where **W** is a weighting matrix.

This is to minimize the mean square errors between the true channel responses and the weighted least square solutions. In other words, MMSE is to find $\hat{\mathbf{H}}_{LMMSE} = \mathbf{W}\hat{\mathbf{H}}_{\mathrm{LS}}$ such that $E\{\left\|\mathbf{H} - \hat{\mathbf{H}}_{LMMSE}\right\|^2\}$ is minimized, where $\hat{\mathbf{H}}=[\hat{H}(0)\ \hat{H}(1)\ \hat{H}(2)\ \cdots \hat{H}(N-1)]^T$ and $\hat{\mathbf{H}}_{LS} = [\hat{H}_{LS}(0)\ \ \hat{H}_{LS}(1)\ \ \hat{H}_{LS}(2)\ \cdots \hat{H}_{LS}(M-1)]^T$. By orthogonality property, the MMSE channel estimator can be derived as the following

$$\begin{aligned} &\Rightarrow E\{(\mathbf{H} - \mathbf{W}\hat{\mathbf{H}}_{\mathrm{LS}})^H \hat{\mathbf{H}}_{LS}\}=0 \\ &\Rightarrow E\{\mathbf{H}^H \hat{\mathbf{H}}_{LS}\}_{\mathrm{N\times M}} = \mathbf{W}^H E\{\hat{\mathbf{H}}_{LS}^H \hat{\mathbf{H}}_{\mathrm{LS}}\}_{M\times M} \\ &\Rightarrow \mathbf{W}^H = \mathbf{R}_{\mathbf{H}\hat{\mathbf{H}}_{\mathrm{LS}}} \mathbf{R}^{-1}_{\hat{\mathbf{H}}_{\mathrm{LS}}} = \mathbf{R}_{\mathbf{H}\mathbf{H}_{\mathrm{LS}}} \mathbf{R}^{-1}_{\hat{\mathbf{H}}_{\mathrm{LS}}} \end{aligned} \tag{2.17}$$

where

$$\mathbf{R}_{\mathbf{H}\hat{\mathbf{H}}_{LS}} = E\{\mathbf{H}(\mathbf{H}_{LS} + \tilde{\mathbf{Z}})^H\} = E\{\mathbf{H}\mathbf{H}_{LS}^H\} = \mathbf{R}_{\mathbf{H}\mathbf{H}_{LS}}$$

$$\mathbf{R}_{\hat{\mathbf{H}}_{LS}} = E\{\mathbf{H}_{LS}\mathbf{H}_{LSLS}^H\} + E\{\tilde{\mathbf{Z}}\tilde{\mathbf{Z}}^H\} = \mathbf{R}_{\mathbf{H}_{LS}} + E\{\tilde{\mathbf{Z}}\tilde{\mathbf{Z}}^H\}$$

$$\tilde{\mathbf{Z}} = \left[\tilde{Z}_0\ \ \tilde{Z}_1 \cdots \tilde{Z}_{M-1}\right]^T = \left[\frac{Z_0}{P_0}\ \ \frac{Z_1}{P_1}\ \ \cdots \frac{Z_{M-1}}{P_{M-1}}\right]$$

P_k : the pilot of the k-th subcarrier

If noises are independent and all pre-known data have the same power, that is $|\mathrm{P}_k| = p, k = 0,1,\cdots,M-1$, and variance of the AWGN is σ_Z^2 then

$$\mathbf{R}_{\hat{\mathbf{H}}_{LS}} = \mathbf{R}_{\mathbf{H}_{LS}} + \frac{\sigma_Z^2}{p^2}\mathbf{I} \tag{2.18}$$

Therefore, the MMSE channel estimator can be formulated as

$$\hat{\mathbf{H}}_{MMSE} = \mathbf{W}\hat{\mathbf{H}}_{LS} = \mathbf{R}_{\mathbf{H}\mathbf{H}_{LS}}(\mathbf{R}_{\mathbf{H}_{LS}} + \frac{\sigma_z^2}{p^2}\mathbf{I})^{-1}\hat{\mathbf{H}}_{LS} \tag{2.19}$$

Note that the channel statistics $\mathbf{R}_{\mathbf{H}\mathbf{H}_{LS}}$ and $\mathbf{R}_{\mathbf{H}_{LS}}$ are required in the MMSE estimator. If the subcarriers are very close to each other, then the frequency domain correlation can be used to interpolate the complete channel responses, even if pilots are not known for all subcarriers. The coherent bandwidth of the channel is usually approximated to the inverse of the delay spread [5]. If the subcarrier spacing is much less than the coherent bandwidth, the frequency responses of the channels on neighboring subcarriers can be considered identical. There are many well-known process of interpolation, such as linear interpolation, polynomial interpolation, cubic spline interpolation. In the following section, a DFT-based 1-Dimension channel interpolator will be introduced.

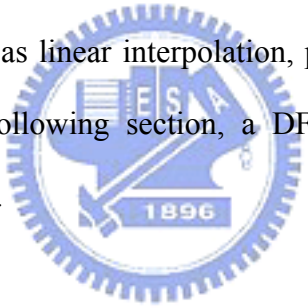

2.3.3 DFT-based 1-Dimension Channel Estimator [11]

DFT-based channel estimators were proposed in [11] [12]. In this section, a DFT-based 1-D channel estimator will be proposed. Compared with the LMMSE estimator, the DFT-based channel estimator has low complexity but has some restrictions on pilot locations. If pilots are equal-spaced and the channel delay spread is less than the total number of pilots, then the complete channel impulse responses can be interpolated exactly based on pilot tones. Detail mathematic descriptions will be presented in the following.

Discrete Fourier Transform (DFT) and Inverse Discrete Fourier Transform (IDFT) pairs of the channel response can be illustrated as

$$H[k]=\sum_{n=0}^{N-1}h[n]e^{-\frac{2\pi kn}{N}},k=0,1,\cdots,N-1$$
$$h[n]=\frac{1}{N}\sum_{k=0}^{N-1}H[k]e^{j\frac{2\pi kn}{N}},n=0,1,\cdots,N-1 \quad (2.20)$$

where $H[k]$ is the frequency responses of the *k*-th subcarrier, and $h[n]$ is the channel responses of the *n*-th sample.

If pilots are equal-spaced, the frequency responses of pilot subcarriers are described as

$$H_p(k)=H(kN_s),k=0,1,2,\cdots,\frac{N}{N_s}-1 \quad (2.21)$$

where N_s is the duration of pilot spacing.

Assume $\frac{N}{N_s}$ is an integer, then $\frac{N}{N_s}$-points IDFT of $H_p(k)$ is as

$$\begin{aligned}
h_p[n]&=\frac{1}{\frac{N}{N_s}}\sum_{k=0}^{\frac{N}{N_s}-1}H_p(k)e^{j\frac{2\pi kn}{\frac{N}{N_s}}},n=0,1,2,\cdots,\frac{N}{N_s}-1\\
&=\frac{1}{\frac{N}{N_s}}\sum_{k=0}^{\frac{N}{N_s}-1}H(kN_s)e^{j\frac{2\pi kn}{\frac{N}{N_s}}}\\
&=\frac{1}{\frac{N}{N_s}}\sum_{k=0}^{\frac{N}{N_s}-1}\left(\sum_{m=0}^{N-1}h[m]e^{-j\frac{2\pi(kN_s)m}{N}}\right)e^{j\frac{2\pi kn}{\frac{N}{N_s}}}\\
&=\sum_{m=0}^{N-1}h[m]\left(\frac{1}{\frac{N}{N_s}}\sum_{k=0}^{\frac{N}{N_s}-1}e^{-\frac{2\pi(m-n)k}{\frac{N}{N_s}}}\right)\\
&=\sum_{m=0}^{N-1}h[m]\delta(m-n)\\
&=h[n],n=0,1,2,\cdots,\frac{N}{N_s}-1
\end{aligned} \quad (2.22)$$

Observe the results of eq. (2.22), we can conclude that:

If the length of the channel responses $h[n]$ are less then $\frac{N}{N_s}$, then $h[n]$ are

complete identical to $\frac{N}{N_s}$-points IDFT of $H_p(k)$ at the first $\frac{N}{N_s}$ points. Therefore, adding $N-\frac{N}{N_s}$ points of zeros to the last of $h_p[n]$, total channel responses $h[n], n=0,1,2,\cdots,N-1$ can be obtained.

In general, the frequency responses of the pilot tones can be estimated by the LS channel estimator (section 2.3.1), and the DFT-based interpolation is used to acquire all channel responses.

2.3.4 Channel Estimator Based on A Time Domain Correlation [10] [17]

Time domain correlation channel estimators are often used to estimate multipath gains with the preamble for the initial channel estimation. If the cyclic autocorrelation function of the preamble is a Kronecker delta function, then the time domain path gain can be estimated simply by calculating the cyclic cross correlation between the preamble and the received signals. However, there are some restrictions on the preamble sequences.

The cyclic autocorrelation function of the preamble can be calculated as

$$r_{pp}[l]=\sum_{n=0}^{n=N-1} p^*[n]p[(n-l)_N], l=0,1,\cdots,N-1 \qquad (2.23)$$

where $p[n]$ is the preamble samples, superscript * means complex conjugate, $(n)_N$ means (n modulo N) , and N is the length of the preamble. The notation in the following equations is identical.

The cyclic cross correlation between the preamble and the received signals can be calculated as

$$r_{yp}[l]=\sum_{n=0}^{n=N-1} y^*[n]p[(n-l)_N], l=0,1,\cdots,N-1 \qquad (2.24)$$

where $y[n]$ is the received signal samples

If $r_{pp}[l]$ is a Kronecker delta function, that is

$$r_{pp}[l] = \sum_{n=0}^{n=N-1} p^*[n]p[(n-l)_N] = \begin{cases} 1, l = 0 \\ 0, l \neq 0 \end{cases} \tag{2.25}$$

Then the path gain with delay l can be calculated as

(Noise free case and CP length > delay spread is assumed)

$$h[l] = r_{pp}[l] = r_{yp}[l] = \sum_{n=0}^{n=N-1} y^*[n]p[(n-l)_N],\ l = 0,1,\cdots,N-1 \tag{2.26}$$

If $r_{pp}[l]$ is not a Kronecker delta function, assume $\mathbf{Q}$ is formed by auto-correlation of the preabmle as

$$\mathbf{Q} = \begin{bmatrix} r_{pp}[0] & r_{pp}[1] & \cdots & r_{pp}[L-1] \\ r_{pp}[-1] & r_{pp}[0] & \cdots & r_{pp}[L-2] \\ \vdots & \vdots & \ddots & \vdots \\ r_{pp}[-L+1] & r_{pp}[-L+2] & \cdots & r_{pp}[0] \end{bmatrix} \tag{2.27}$$

Let $\mathbf{r}_{yp}$ be a vector formed by the cross-correlation between the received signals and the preamble as

$$\mathbf{r}_{yp} = \begin{bmatrix} r_{yp}[0] & r_{yp}[1] & r_{yp}[2] & \cdots & r_{yp}[L-1] \end{bmatrix}^T \tag{2.28}$$

Then the estimated path gain can be solved by

$$\tilde{\mathbf{h}} = \begin{bmatrix} \tilde{h}[0] & \tilde{h}[1] & \cdots \tilde{h}[L-1] \end{bmatrix}^T = \mathbf{Q}^{-1}\mathbf{r}_{yp} \tag{2.29}$$

However, if noises are considered

$$\begin{aligned} r_{yp}[l] &= \sum_{n=0}^{n=N-1} y^*[n]p[(n-l)_N] \\ &= \sum_{n=0}^{n=N-1} (p[n] \otimes_N h[n])p^*[(n-l)_N] + z[n]p^*[(n-l)_N] \\ &= \sum_{n=0}^{N-1} r_{pp}[n-l]h[l] + \tilde{z}[l] \end{aligned} \tag{2.30}$$

where $z[n]$ represents noise samples and $\tilde{z}[l]=\sum_{n=0}^{N-1} z[n]p^{*}[(n-l)_N]$

then eq. (2.29) will be

$$\tilde{\mathbf{h}} = \mathbf{Q}^{-1}\mathbf{r}_{yp} = \mathbf{Q}^{-1}(\mathbf{Q}\mathbf{h}+\tilde{\mathbf{z}}) = \mathbf{h}+\mathbf{Q}^{-1}\tilde{\mathbf{z}} = \mathbf{h}+\hat{\mathbf{z}} \tag{2.31}$$

where $\mathbf{r}_{pp} = [r_{pp}[0]\ r_{pp}[1]\ \cdots\ r_{pp}[\mathrm{L}-1]]^T$, $\tilde{\mathbf{z}} = \left[\tilde{z}[0]\ \tilde{z}[1]\ \cdots \tilde{z}[L-1]\right]^T$ and

$\hat{\mathbf{z}} = \left[\hat{z}[0]\ \hat{z}[1]\ \cdots \hat{z}[L-1]\right]^T = \mathbf{Q}^{-1}\tilde{\mathbf{z}}$

Therefore, enhancement noises power can be calculated as

$$\begin{aligned} E\{\hat{\mathbf{z}}^H\hat{\mathbf{z}}\} &= E\{(\mathbf{Q}^{-1}\tilde{\mathbf{z}})^H(\mathbf{Q}^{-1}\tilde{\mathbf{z}})\} \\ &= E\{tr(\tilde{\mathbf{z}}^H(\mathbf{Q}^{-1})^H\mathbf{Q}^{-1}\tilde{\mathbf{z}})\} \\ &= E\{tr(\mathbf{Q}^{-1}\tilde{\mathbf{z}}\tilde{\mathbf{z}}^H(\mathbf{Q}^{-1})^H)\} \\ &= tr(E\{\mathbf{Q}^{-1}\tilde{\mathbf{z}}\tilde{\mathbf{z}}^H(\mathbf{Q}^{-1})^H\}) \\ &= \sigma_{\tilde{z}}^2 tr(\mathbf{Q}^{-1}(\mathbf{Q}^{-1})^H) \\ &= \sigma_{\tilde{z}}^2 \sum_{i=0}^{L-1}\sum_{j=0}^{L-1}(\mathbf{Q}^{-1})_{ij}^2 \end{aligned} \tag{2.32}$$

Therefore, noises are enhanced by a factor of $\sum_{i=0}^{L-1}\sum_{j=0}^{L-1}(\mathbf{Q}^{-1})_{ij}^2$ which strongly depends on the structure of $\mathbf{Q}$.

2.3.5 Decision Feedback or Decision Directed Channel Estimator

In decision direct (DD) channel estimator, data are detected based on the channel responses of the previous OFDM symbol, and then the decision data are as virtual pilots to estimate the current channel responses. DD channel estimators are quite bandwidth efficiency because no pilots are transmitted. However, the channel responses of successive OFDM symbols must remain static to ensure the correctness of the decision data. Otherwise, error propagation problems can not be avoided and

the variation between successive channels will degrade the performance of the DD channel estimators. In order to compensate the variation between successive channels, some kinds of tracking algorithms can be applied.

Chapter 3
Semi-blind Channel Estimator with Sparse Pilots for High Mobility OFDM Systems

The proposed semi-blind channel estimator is presented in this chapter. In the beginning, the initial channel estimator based on multipath interference cancellation (MPIC) is presented. Then, the adaptive Newton tracking methods for the following OFDM symbols are introduced.

3.1 System Description

OFDM systems are considered and equivalent baseband QPSK transmitted and received signals are described as:

Transmitted signals: N QPSK Symbols $X_k \in \{\pm 1 \pm j\}, k = 0 \cdots N-1$

Channel model: $H_k = \sum_{l=0}^{\zeta-1} h_l e^{-j\frac{2\pi k \tau_l}{N}}, k = 0,1,\cdots,N-1$

Received signal: $Y_k = Y_{kI} + jY_{kQ} = H_k X_k + Z_k, k = 0 \cdots N-1$ (3.1)

where Z_k are additive white Gaussian noises (AWGN), H_k is the channel frequency responses of the k-th subcarrier, τ_l is the time delay of the l-th path, ζ is the number of multipaths, and N is the number of used subcarriers.

3.1.1 OFDM Packet Format

General OFDM packets can be formulated as Fig. 3.1. The initial channel is estimated with preamble and the channels of the following P OFDM symbols are estimated by some kinds of tracking algorithm.

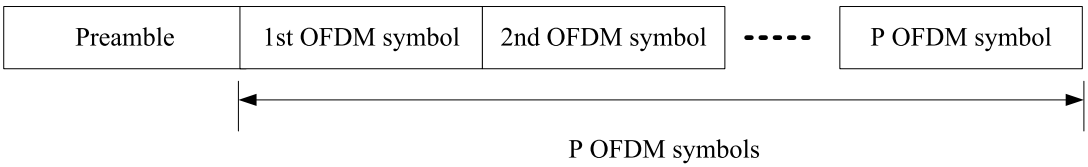

Figure 3.1 OFDM packet format

In this chapter, the time domain channel estimator based on multipath interference cancellation (MPIC) will be proposed to estimate the initial channel with the preamble defined in IEEE 802.16 standard. Following the initial channel estimation, the adaptive Newton method will be used to track the channels of the following *P* OFDM symbols. The flow chart of the proposed channel estimation methods are illustrated in Fig. 3.2. Details will be discussed in the following sections.

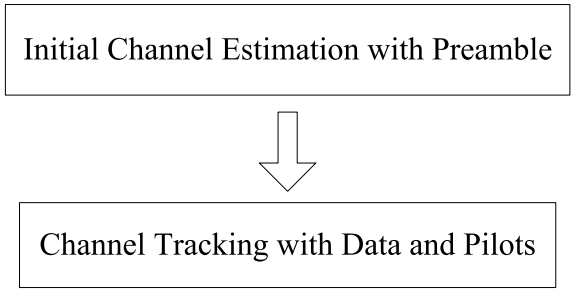

Figure 3.2 Flow chart of the proposed semi-blind channel estimation

3.2 Initial Channel Estimation Based on Multipath Interference Cancellation (MPIC)

In real communication systems, guard bands are defined to avoid interferences between different systems. As described in the previous section, guard bands of 55 subcarriers are defined in IEEE 802.16 standard. Lacking of high frequency information, the cyclic-shift-autocorrelation function of the preamble can not be ideal impulse. Due to the imperfect cyclic-shift-autocorrelation of the preamble, the performance of the time domain correlation channel estimator is affected by multipath interference problems [10], [17]. Therefore, in order to obtain the initial time domain impulse responses with the preamble, special designs are needed. In this section, the time domain channel estimator based on multipath interference cancellation (MPIC) will be proposed.

First, the cyclic-shift auto-correlation function is our concern. Normalized cyclic-shift auto-correlation can be calculated as

$$r_{pp}[\tau] = \frac{\sum_{n=0}^{N-1} p^*[n]p[(n-\tau)_N]}{\sum_{n=0}^{N-1} p^*[n]p[n]}, \tau = 0,1,\cdots,N-1 \qquad (3.2)$$

where $p[n]$ is the time domain preamble sequence,the notaion $(n)_N$ denotes (n modulo N) and $p[(n-\tau)_N]$ is the right cyclic-shift τ of $p[n]$.

The proposed time domain channel estimator with the preamble based on multipath interference cancellation (MPIC) methods is divided into two phases. In the phase I, multipath gains are estimated path-by-path by canceling only the pre-estimated path interferences. In the phase II, the multipath gains are refined path-by-path by canceling all the estimated interferences.

Calculate the normalized auto-correlation of the preamble before implementing the estimator algorithm as

$$r[\tau_l] = \frac{\sum_{n=0}^{n=255} p^*[n]p[(n-\tau_l)_{256}]}{\sum_{n=0}^{n=255} p^*[n]p[n]}, \tau_l = 1,\cdots,127 \quad (3.3)$$

where $p[n]$ means preamble samples and $(n-\tau)_N$ means ($(n-\tau)$ modulo *N*). Eq. (3.3) is a special case when *N*=128 in the eq. (3.2)

Phase I algorithm is illustrated in the following:

Phase I:

Calculate the cross-correlation between the received signals and the preamble and find the delay with maximal power to locate the largest path in the step 1 as

Step1:

$$r_{yp}[\tau] = \sum_{n=0}^{n=255} y[n]^* p[(n-\tau)_{256}],\ \tau = 0,1,\cdots,L<128 \quad (3.4)$$

$$m[\tau_l] = \arg\max_{r_{yp}[\tau]} \{|r_{yp}[\tau]|^2\},\ \tau = 0,1,\cdots,L<128 \quad (3.5)$$

where y[n] are the time domain received signal samples, $p[n]$ are the time domain preamble samples, $r_{yp}[\tau]$ are the cross-correlation between the received signal and the preamble samples, $m[\tau_l]$ is the estimated gain of the l-th path with time delay τ_l. L is the length of the observation window.

Cancel the maximal path interferences from $r_{yp}(\tau)$, and find the delay with maximal power to locate a new path in the step 2 as

Step 2:

$$r'_{yp}[\tau] = r_{yp}[\tau] - m[\tau_l]r[|\tau-\tau_l|], \tau = 0,1,\cdots,L, \text{and } 0<|\tau-\tau_l|<128 \quad (3.6)$$

$$m[\tau_l] = \arg\max_{r'_{yp}[\tau]} \{|r'_{yp}[\tau]|^2\},\ \tau = 0,1,\cdots,L \neq \text{ all } \tau_l \text{ finded before} \quad (3.7)$$

The step 3 is as

Step 3:

Let $r_{yp}[\tau] = r'_{yp}[\tau]$, and repeat Step 2 until N_p paths are estimated

where N_p is the path number in the estimator

In the phase I, the observation window length L is set to 63 (the length of CP is 64).

Phase II: Refine the path gains and path delays.

Coarse path gains $m[\tau_l]$ and path delay τ_l, $l = 0,1,\cdots,N_p$ are estimated in the phase I. In the phase II, the larger $\left[\frac{N_p}{2}\right]$ paths are estimated by cancelling the larger $\left[\frac{N_p}{2}\right]-1$ path interferences from $r_{yp}(\tau)$ and the other $N_p - \left[\frac{N_p}{2}\right]$ paths are estimated by cancelling all the path interferences with larger path gains. The pseudo code of the phase II algorithm is presented in the appendix.

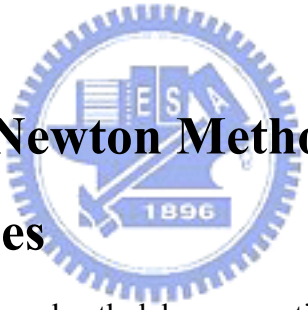

3.3 An Adaptive Newton Method to Track Channel Responses

After the initial path gains and path delays are estimated in the initial channel estimator, the channel responses of the following *P* OFDM symbols are tracked by adaptive Newton methods in the time domain. Adaptive Newton method will be introduced in this section.

3.3.1 Channel Estimator Model

Recall eq. (3.1), the channel frequency responses are modeled as

$$H_k = \sum_{l=0}^{\zeta-1} h_l e^{-j\frac{2\pi k\tau_l}{N}}, k = 0,1,\cdots,N-1$$

where k is subcarrier index, h_l is the complex channel gain of the l-th path, τ_l is the time delay of the l-th path, and ζ is the number of multipaths.

The proposed channel estimator model in the frequency domain is described as

$$
\begin{aligned}
M_k &= \sum_{l=0}^{L-1} m_l e^{-j\frac{2\pi k\tau_l}{N}} = \sum_{l=0}^{L-1} (a_l + jb_l) e^{-j\frac{2\pi k\tau_l}{N}}, k = 0,1,\cdots,N-1 \\
&= (\sum_{l=0}^{L-1} (a_l \cos(\frac{2\pi k\tau_l}{N}) + \sum_{l=0}^{L-1} (b_l \sin(\frac{2\pi k\tau_l}{N})) + \\
&\quad j(\sum_{l=0}^{L-1} (b_l \cos(\frac{2\pi k\tau_l}{N}) - \sum_{l=0}^{L-1} (a_l \sin(\frac{2\pi k\tau_l}{N}))) \\
&= M_{kI} + jM_{kQ}
\end{aligned}
\tag{3.8}
$$

where M_k is the estimated frequency responses of the *k*-th subcarrier, m_l is the estimated complex gain of the *l*-th path in the time domain, τ_l is the time delay of the *l*-th path, and *L* is the number of multipaths in this proposed channel model(equal to the number of the legal paths after initial channel estimators). a_l is the real part of *l*-th path and b_l is the imaginary part of *l*-th path

3.3.2 Problems Formulation

Assume the multipath delay τ_l are estimated with the preamble in the initial channel estimation and remain constant during one transmission packet, then Maximal Likelihood (ML) criterion to estimate the channel responses can be represented as

$$
\{\hat{\mathbf{X}}, \hat{\mathbf{H}}\} = \arg\min_{\{\hat{\mathbf{X}}, \hat{\mathbf{H}}\}} \{\sum_{k=0}^{N-1} |Y_k - H_k X_k|^2\} = \arg\min_{\{\hat{\mathbf{H}}\}} \min_{\{\hat{\mathbf{X}}\}} \{\sum_{k=0}^{N-1} |Y_k - H_k X_k|^2\} \tag{3.9}
$$

where $\{\mathbf{X}, \mathbf{H}\} = \{X_0, X_1, \cdots X_{N-1}, H_0, H_1, \cdots, H_{N-1}\}$

The second minimization in eq. (3.9) can be achieved with the LS solution if channel is known and the channel estimation problem becomes

$$
\begin{aligned}
\{\hat{a}_0, \cdots, \hat{a}_{L-1}, \hat{b}_0, \cdots, \hat{b}_{L-1}\} &= \arg\min_{\{a_0, \cdots, a_{L-1}, b_0, \cdots, b_{L-1}\}} \{\sum_{k=0}^{N-1} |Y_k - M_k \hat{X}_k|^2\} \\
&= \arg\min_{\{a_0, \cdots, a_{L-1}, b_0, \cdots, b_{L-1}\}} f(a_0, \cdots, a_{L-1}, b_0, \cdots, b_{L-1})
\end{aligned}
\tag{3.10}
$$

where $f(a_0, \cdots, a_{L-1}, b_0, \cdots, b_{L-1}) = \sum_{k=0}^{N-1} |Y_k - M_k \hat{X}_k|^2$ and $\hat{X}_k$ is the decision signals

based on the channel responses of the estimator. Decision signals $\hat{X}_k$ can be written as

$$\begin{aligned}\hat{X}_k &= decision\{\frac{Y_k}{M_k}\} = sign(Y_{kI}M_{kI} + Y_{kQ}M_{kQ}) + jsign(Y_{kQ}M_{kI} - Y_{kI}M_{kQ}) \\ &= sign(\alpha_k) + \text{jsign}(\beta_k)\end{aligned} \tag{3.11}$$

where *decision* means make hard decision, $\alpha_k = Y_{kI}M_{kI} + Y_{kQ}M_{kQ}$, $\beta_k = Y_{kQ}M_{kI} - Y_{kI}M_{kQ}$ and the *sign* function is defined as

$$sign(x) = \begin{cases} 1 & , x \geq 0 \\ -1 & , x < 0 \end{cases} \tag{3.12}$$

From eq. (3.10)-(3.12), the fucntion $f(a_0, \cdots, a_{L-1,} b_0, \cdots, b_{L-1})$ can be rearranged as

$$f(a_0, \cdots, a_{L-1,} b_0, \cdots, b_{L-1}) = \sum_{k=0}^{N-1} \{r_k^{\,2} + s_k^{\,2}\} \tag{3.13}$$

where

$$\begin{aligned} r_k &= Y_{kI} - M_{kI} sign(\alpha_k) + M_{kQ} sign(\beta_k); \\ s_k &= Y_{kQ} - M_{kQ} sign(\alpha_k) - M_{kI} sign(\beta_k); \end{aligned} \tag{3.14}$$

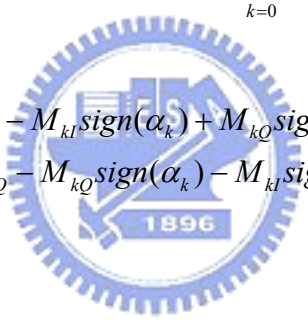

3.3.3 Adaptive Newton Methods

Before continuing the proposed channel tracking method, we introduce the Newton method to optimize a certain target function. Newton method is an adaptive method to find a solution of input parameters such that the target function is minimized. Newton methods can be described as

$$\begin{aligned} &\text{Target function } f(\mathbf{x}) : R^N \to R \\ &\text{to find } \mathbf{x} \text{ such that } f(\mathbf{x}) \text{ is minimal} \\ &\text{Newton method: } \mathbf{x}^{(k+1)} = \mathbf{x}^{(k)} - (\lambda \mathbf{I}_N + Hessian(f(\mathbf{x}^{(k)})))^{-1} \nabla f(\mathbf{x}^{(k)}) \end{aligned} \tag{3.15}$$

where $f(\mathbf{x})$ is the target function from R^N to R , $\mathbf{x}^{(k)}$ is the vector of the *k*-th iteration, $Hessian(f(\mathbf{x}^{(k)}))$ represents the Hessian matrix of $f(\mathbf{x}^{(k)})$, $\nabla f(\mathbf{x}^{(k)})$

represents the gradient vector of $f(\mathbf{x}^{(k)})$, λ is a constant to ensure existence of the inverse function.

Go back to the proposed channel estimator model, the channel tracking problems can be described as:

Let $f(\mathbf{x}) = f(a_0,\cdots,a_{L-1,}b_0,\cdots,b_{L-1}) = \sum_{k=0}^{N-1}\{r_k^{\,2} + s_k^{\,2}\}$ to be the target function, in order to track the time domain path gains $\mathbf{x} = [a_0,\cdots,a_{L-1,}b_0,\cdots,b_{L-1}]^T$ such that the target function $f(a_0,\cdots,a_{L-1,}b_0,\cdots,b_{L-1})$ is minimized.

If the gradient vector and Hessian matrix of $f(\mathbf{x}) = f(a_0,\cdots,a_{L-1,}b_0,\cdots,b_{L-1})$ is calculated , then the Newton method can be used to track the channel path gains. The solutions will be showed in the following.

From eq. (3.13), the *j*-th term of the gradient vector is calculated as

$$(\nabla f(\mathbf{x}))_j = \frac{\partial f(\mathbf{x})}{\partial x_j} = 2\sum_{i=1}^{N-1}\{r_i(\mathbf{x})\frac{\partial r_i(\mathbf{x})}{\partial x_j} + s_i(\mathbf{x})\frac{\partial s_i(\mathbf{x})}{\partial x_j}\} \tag{3.16}$$

Moreover, the *k*-th row, *j*-th column of the Hessian matrix can be calculated as

$$\begin{aligned}
&Hessian(f(\mathbf{x}))_{kj} = \frac{\partial^2 f(\mathbf{x})}{\partial x_k \partial x_j} \\
&= \frac{\partial}{\partial x_k}(\frac{\partial f(\mathbf{x})}{\partial x_j}) = \frac{\partial}{\partial x_k}(2\sum_{i=1}^{N-1}\{r_i(\mathbf{x})\frac{\partial r_i(\mathbf{x})}{\partial x_j} + s_i(\mathbf{x})\frac{\partial s_i(\mathbf{x})}{\partial x_j}\}) \\
&=2\sum_{\mathrm{i}=1}^{N\text{-}1}\frac{\partial r_i(\mathbf{x})}{\partial x_k}\frac{\partial r_{\mathrm{i}}(\mathbf{x})}{\partial x_j} + r_i(\mathbf{x})\frac{\partial^2 r_i(\mathbf{x})}{\partial x_k \partial x_j} + 2\sum_{\mathrm{i}=1}^{N\text{-}1}\frac{\partial s_i(\mathbf{x})}{\partial x_k}\frac{\partial s_i(\mathbf{x})}{\partial x_j} + s_i(\mathbf{x})\frac{\partial^2 s_i(\mathbf{x})}{\partial x_k \partial x_j} \\
&\simeq 2\sum_{\mathrm{i}=1}^{N\text{-}1}\frac{\partial r_i(\mathbf{x})}{\partial x_k}\frac{\partial r_{\mathrm{i}}(\mathbf{x})}{\partial x_j} + 2\sum_{\mathrm{i}=1}^{N\text{-}1}\frac{\partial s_i(\mathbf{x})}{\partial x_k}\frac{\partial s_i(\mathbf{x})}{\partial x_j}
\end{aligned} \tag{3.17}$$

From eq.(3.16), (3.17), when $\frac{\partial r_k}{\partial a_l}, \frac{\partial r_k}{\partial b_l}, \frac{\partial s_k}{\partial a_l}, \frac{\partial s_k}{\partial b_l}$ are calculated by partial differential, then the gradient vector and Hessian matrix of $f(\mathbf{x})$ can be calculated as

$$\begin{aligned}
\frac{\partial r_k}{\partial a_l} &= -(\frac{\partial M_{kI}}{\partial a_l}sign(\alpha_k) + M_{kI}\frac{\partial sign(\alpha_k)}{\partial a_l}) + (\frac{\partial M_{kQ}}{\partial a_l}sign(\beta_k) + M_{kQ}\frac{\partial sign(\beta_k)}{\partial a_l}) \\
&= -\cos(\frac{2\pi k\tau_l}{N})sign(\alpha_k) - \sin(\frac{2\pi k\tau_l}{N})sign(\beta_k)
\end{aligned}$$

$$\frac{\partial r_k}{\partial b_l} = -(\frac{\partial M_{kI}}{\partial b_l} sign(\alpha_k) + M_{kI} \frac{\partial sign(\alpha_k)}{\partial b_l}) + (\frac{\partial M_{kQ}}{\partial b_l} sign(\beta_k) + M_{kQ} \frac{\partial sign(\beta_k)}{\partial b_l})$$
$$= -\sin(\frac{2\pi k\tau_l}{N}) sign(\alpha_k) + \cos(\frac{2\pi k\tau_l}{N}) sign(\beta_k)$$
$$\frac{\partial s_k}{\partial a_l} = -(\frac{\partial M_{kQ}}{\partial a_l} sign(\alpha_k) + M_{kQ} \frac{\partial sign(\alpha_k)}{\partial a_l}) - (\frac{\partial M_{kI}}{\partial a_l} sign(\beta_k) + M_{kI} \frac{\partial sign(\beta_k)}{\partial a_l})$$
$$= \sin(\frac{2\pi k\tau_l}{N}) sign(\alpha_k) - \cos(\frac{2\pi k\tau_l}{N}) sign(\beta_k)$$
$$\frac{\partial s_k}{\partial b_l} = -(\frac{\partial M_{kQ}}{\partial b_l} sign(\alpha_k) + M_{kQ} \frac{\partial sign(\alpha_k)}{\partial b_l}) - (\frac{\partial M_{kI}}{\partial b_l} sign(\beta_k) + M_{kI} \frac{\partial sign(\beta_k)}{\partial b_l})$$
$$= -\cos(\frac{2\pi k\tau_l}{N}) sign(\alpha_k) - \sin(\frac{2\pi k\tau_l}{N}) sign(\beta_k)$$

(3.18)

Note that in the above differential, the probability of $\alpha_k = 0$ (or $\beta_k = 0$) are assumed zero.

Therefore, from eq. (3.16), (3.17), (3.18), the Newton method for target function of (3.13) can be obtained.

The procedure of Newton tracking is summarized as: Firstly, initial data decisions are based on the channel responses of the previous OFDM symbol, then the path gains are tracked by the Newton methods.

3.3.4 Combination of Pilots and Decision Data Direction

If the variation of the channels between two adjacent OFDM symbols is large, the data decisions based on the channel of the previous channel may have little accuracy. If the tracking direction depends only on the decision data, error propagation problems may dominate the accuracy of the channel estimator. In order to obtain more accurate tracking direction, the combination direction of the pilots and decision data is used for the first Newton tracking iteration.

The pilot direction is introduced in the following:

There are 8 pilots in IEEE 802.16 standard (not equal spaced, listed in Table 4.1). The maximal likelihood criterion of the channel response based on pilot subcarriers can be represented as

$$\begin{aligned}
\{\hat{\mathbf{a}},\hat{\mathbf{b}}\} &= \underset{\{a_0,a_1,\cdots a_{L-1},b_0,b_1,\cdots b_{L-1}\}}{\arg\min} \{\sum_{k\in\mathbf{J}} \left|P_k M_k - Y_k\right|^2\} \\
&= \underset{\{a_0,a_1,\cdots a_{L-1},b_0,b_1,\cdots b_{L-1}\}}{\arg\min} \{\sum_{k\in\mathbf{J}} \left|P_k \sum_{l=0}^{L-1}(a_l + jb_l)e^{-j\frac{2\pi k\tau_l}{N}} - Y_k\right|^2\} \\
&= \underset{\{a_0,a_1,\cdots a_{L-1},b_0,b_1,\cdots b_{L-1}\}}{\arg\min} \{\sum_{k\in\mathbf{J}} \left|P_k\right|^2 \left|\sum_{l=0}^{L-1}(a_l + jb_l)e^{-j\frac{2\pi k\tau_l}{N}} - \frac{Y_k}{P_k}\right|^2\} \\
&= \underset{\{a_0,a_1,\cdots a_{L-1},b_0,b_1,\cdots b_{L-1}\}}{\arg\min} \{\sum_{k\in\mathbf{J}} \left|\sum_{l=0}^{L-1}(a_l + jb_l)e^{-j\frac{2\pi k\tau_l}{N}} - \frac{Y_k}{P_k}\right|^2\}
\end{aligned} \tag{3.19}$$

where P_k is the pilot of the k-th subcarrier and $\mathbf{J}$ = {-88,-63,-38,-13,13,38,63,88} which is the same as the locations defied in IEEE 802.16 OFDM mode

Let the target function be

$$f(\mathbf{x}_p) = f(a_0,\cdots,a_{L-1},b_0,\cdots,b_{L-1}) = \sum_{k\in\mathbf{J}} \left|\sum_{l=0}^{L-1}(a_l + jb_l)e^{-j\frac{2\pi k\tau_l}{N}} - \hat{H}_k\right|^2 \tag{3.20}$$

where the subindex p of $\mathbf{x}_p$ means pilot and $\hat{H}_k = \frac{Y_k}{P_k}$

The gradient vector of $f(\mathbf{x}_p)$ is calculated as

$$\begin{aligned}
\left.\frac{\partial f(\mathbf{x}_p)}{\partial a_l}\right|_{a_l=a_{l,t-1}} &= 2\sum_{k\in\mathbf{J}}[((\sum_{l=0}^{L-1} a_{l,t-1}\cos(\frac{2\pi k\tau_l}{N}) + b_{l,t-1}\sin(\frac{2\pi k\tau_l}{N})) - \hat{H}_{kI})\cos(\frac{2\pi k\tau_l}{N}) \\
&\quad -((\sum_{l=0}^{L-1} b_l\cos(\frac{2\pi k\tau_l}{N}) - a_l\sin(\frac{2\pi k\tau_l}{N})) - \hat{H}_{kQ})\sin(\frac{2\pi k\tau_l}{N})] \\
&= 2\sum_{k\in\mathbf{J}}[(\hat{H}_{kI,t-1} - \hat{H}_{kI})\cos(\frac{2\pi k\tau_l}{N}) - (\hat{H}_{kQ,t-1} - \hat{H}_{kQ})\sin(\frac{2\pi k\tau_l}{N})] \\
&= 2\sum_{k\in\mathbf{J}}[\Delta\hat{H}_{kI}\cos(\frac{2\pi k\tau_l}{N}) - \Delta\hat{H}_{kQ}\sin(\frac{2\pi k\tau_l}{N})]
\end{aligned}$$

$$\begin{aligned}
\left.\frac{\partial f(\mathbf{x}_p)}{\partial b_l}\right|_{a_l=a_{l,t-1}} &= 2\sum_{k\in\mathbf{J}}[((\sum_{l=0}^{L-1} a_{l,t-1}\cos(\frac{2\pi k\tau_l}{N}) + b_{l,t-1}\sin(\frac{2\pi k\tau_l}{N})) - \hat{H}_{kI})\sin(\frac{2\pi k\tau_l}{N}) \\
&\quad +((\sum_{l=0}^{L-1} b_{l,t-1}\cos(\frac{2\pi k\tau_l}{N}) - a_{l,t-1}\sin(\frac{2\pi k\tau_l}{N})) - \hat{H}_{kQ})\cos(\frac{2\pi k\tau_l}{N})]
\end{aligned}$$

$$=2\sum_{k\in\mathbf{J}}[(\hat{H}_{kI,t-1}-\hat{H}_{kI})\sin(\frac{2\pi k\tau_l}{N})+(\hat{H}_{kQ,t-1}-\hat{H}_{kQ})\cos(\frac{2\pi k\tau_l}{N})]$$
$$=2\sum_{k\in\mathbf{J}}[\Delta\hat{H}_{kI}\sin(\frac{2\pi k\tau_l}{N})+\Delta\hat{H}_{kQ}\cos(\frac{2\pi k\tau_l}{N})] \tag{3.21}$$

where $\Delta\hat{H}_{kI}=\hat{H}_{kI,t-1}-\hat{H}_{kI}$ and $\Delta\hat{H}_{kQ}=\hat{H}_{kQ,t-1}-\hat{H}_{kQ}$

Recall Newton methods eq. (3.15): $\mathbf{x}^{(k+1)}=\mathbf{x}^{(k)}-(\lambda\mathbf{I}_N+Hessian(f(\mathbf{x}^{(k)})))^{-1}\nabla f(\mathbf{x}^{(k)})$

Define the tracking direction as

$$\Delta f(\mathbf{x}^{(k+1)})=(\lambda\mathbf{I}_N+Hessian(f(\mathbf{x}^{(k)})))^{-1}\nabla f(\mathbf{x}^{(k)}) \tag{3.22}$$

The first iteration direction depends on combination of pilots and decision data direction as

$$\Delta f(\mathbf{x}^{(1)})=\alpha(\beta\left\|\Delta f(\mathbf{x}^{(0)})\right\|\frac{\nabla f(\mathbf{x}_p^{(0)})}{\left\|\nabla f(\mathbf{x}_p^{(0)})\right\|})+(1-\alpha)\Delta f(\mathbf{x}^{(0)}),0\le\alpha\le1 \tag{3.23}$$

where α,β are weighting factors of the direction to adjust the weight between the pilots and decision data.

The directions of the second and latter iterations are only by eq. (3.22).

The flow chart of the proposed channel tracking estimator is illustrated in Fig. 3.3 and Fig. 3.4.

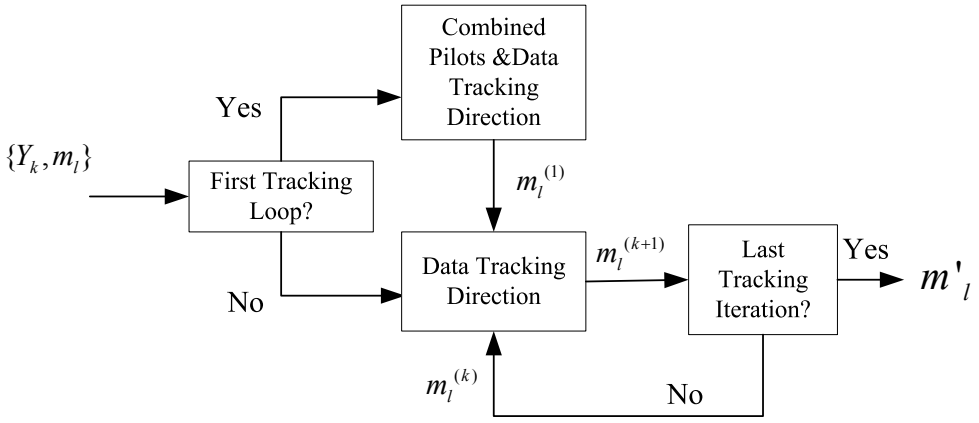

Figure 3.3 Newton methods to track channel impulse responses

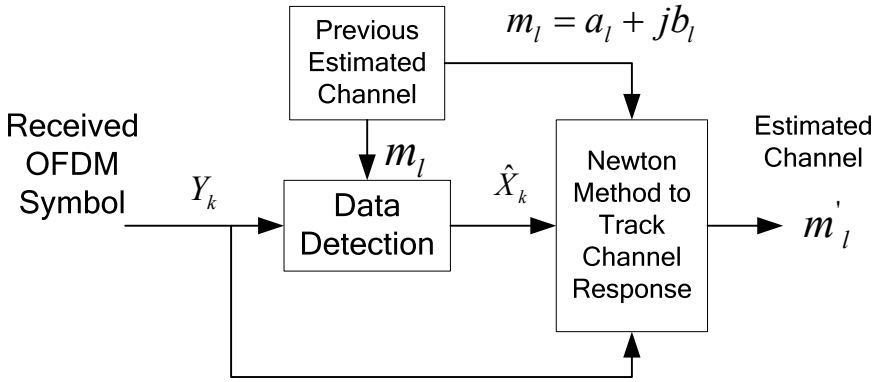

Figure 3.4 Newton methods based on decision data to track channel impulse responses

3.4 Computation Complexity Issues

The computation complexity of the MPIC-based initial channel estimator is calculated in terms of the number of the real multiplications and real additions. The number of multiplication (additions) of N-point $IDFT$ is denoted by $IDFT_{mN}$ $(IDFT_{aN})$. In general, $IDFT_{mN}=IDFT_{aN}=4N\log_2 N$. In the phase I, $r_{yp}[\tau]$ calculated by $r_{yp}[\tau]=IDFT\{Y[k]P[k]\}, k=0,1,\cdots,N-1$ and $\tau=0,,1,\cdots,N-1$. The complexity of operation in the MPIC-based initial channel estimator is listed in Table 3.1 and the total complexity and examples of MPIC-based initial channel estimator is listed in Table 3.2.

	Operation	Real Multiplications	Real Additions
Phase I	$DFT\{y[n]\}$	$4N\log_2 N$	$4N\log_2 N$
	$Y[k]P[k]$	N	0
	$IDFT\{Y[k]P[k]\}$	$4N\log_2 N$	$4N\log_2 N$
	$m[\tau_l]=\arg\max_{r_{yp}[\tau]}\{\lvert r_{yp}[\tau]\rvert^2\}$ $\tau=0,1,\cdots,L$	$2L$	L
	$r'_{yp}[\tau]=r_{yp}[\tau]-m[\tau_l]r[\lvert\tau-\tau_l\rvert]$ $\tau=0,1,\cdots,L$	$2L$	$2L$
Phase II	$r'_{yp}[\tau]=r_{yp}[\tau]-\sum_{k=0,k\neq l}^{\left\lceil\frac{N_p}{2}\right\rceil} m[\tau_k]r([\lvert\tau-\tau_l\rvert])$ $\tau=0,1,\cdots,L$	$2L$*([N_p/2]-1)	$2L$*([N_p/2]-1)
	$m[\tau_l]=\arg\max_{r_{yp}[\tau]}\{\lvert r_{yp}[\tau]\rvert^2\}$ $\tau=0,1,\cdots,L$	$2L$	L
	$r'_{yp}[\tau]=r_{yp}[\tau]-m[\tau_{l-1}]r[\lvert\tau-\tau_{l-1}\rvert]$ $\tau=0,1,\cdots,L$	$2L$	$2L$

Table 3.1 Complexity of operation in the MPIC-based initial channel estimator

	Real Multiplications	Real Additions
Phase I (N=256,L=118, N_p=6)	$2*4N\log_2 N+N+2L+(Np-1)*4L$	2*4$N\log_2 N$+L+(Np-1)*3L
	19236	18272
Phase II (N=256,L=118, N_p=6)	$[N_p/2]*(2L*([N_p/2]-1)+2L)$ $+(N_p-[N_p/2])*(4L)$	$[N_p/2]*(2L([N_p/2]-1)+L)+$ $(N_p-[N_p/2])*(3L)$
	3540	2832

Table 3.2 Complexity of MPIC-based initial channel estimator

The complexity of operation in the adaptive Newton tracking is listed in Table 3.3 and total complexity and examples of the adaptive Newton tracking is listed in Table 3.4. In these tables, $|\mathbf{\Theta}|$ means the number of data subcarriers, $|\mathbf{J}|$ is the number of pilots, $[\bullet]^{-1}_{mN_p}$ ($[\bullet]^{-1}_{aN_p}$) is the multiplication (addition) number needed when calculating $N_p \times N_p$ matrix inversion. Hessian matrix which depends on the path delay is calculated only at the initial stage and used in the tracking stages. In the tracking stages, the pilot direction is calculated only at the fist iteration and the data direction is calculated at the other iterations. One *DFT* is needed to obtain frequency responses which are required in the signal detector.

	Operation	Real Multiplications	Real Additions
$Hessian(f(\mathbf{x}))$	$\frac{\partial r_i(\mathbf{x})}{\partial x_k}$(or $\frac{\partial s_i(\mathbf{x})}{\partial x_k}$)	0	N_p
	$2\sum_{i=1}^{N-1}\frac{\partial r_i(\mathbf{x})}{\partial x_k}\frac{\partial r_i(\mathbf{x})}{\partial x_j}+$ $2\sum_{i=1}^{N-1}\frac{\partial s_i(\mathbf{x})}{\partial x_k}\frac{\partial s_i(\mathbf{x})}{\partial x_j}$	$2N$+1	$2N$-1
$\nabla f(\mathbf{x}^{(0)})$	$r_i(\mathbf{x})$ (or $s_i(\mathbf{x})$)	0	2
	$2\sum_{i=1}^{N-1}\{r_i(\mathbf{x})\frac{\partial r_i(\mathbf{x})}{\partial x_j}+s_i(\mathbf{x})\frac{\partial s_i(\mathbf{x})}{\partial x_j}\}$	$N_p(2N+1)$	$N_p(2N-1)+4N$ $+4NN_p$
$(\lambda\mathbf{I}_N+Hessian(f(\mathbf{x})))^{-1}\nabla f(\mathbf{x}^{(k)})$		$(2N_p)^2$	$(2N_p-1)(2N_p)$
Data direction	$\nabla f(\mathbf{x}^{(k)})$	$(2N_p)(2N+1)$	$4N+N_p(6N-1)$
	$(\lambda\mathbf{I}_N+Hessian(f(\mathbf{x}^{(k)})))^{-1}\nabla f(\mathbf{x}^{(k)})$	$(2N_p)^2$	$(2N_p-1)(2N_p)$
Pilot direction	$\frac{\partial f(\mathbf{x}_p)}{\partial a_l}\Big\vert_{a_l=a_{l,t-1}}$ (or $\frac{\partial f(\mathbf{x}_p)}{\partial b_l}\Big\vert_{a_l=a_{l,t-1}}$)	$4\vert\mathbf{J}\vert$	$2\vert\mathbf{J}\vert$
	$\nabla f(\mathbf{x}_p)$	$2\vert\mathbf{J}\vert*2N_p$	$(2\vert\mathbf{J}\vert-1)*2N_p$
	$\beta\left\Vert\Delta f(\mathbf{x}^{(0)})\right\Vert\frac{1}{\left\Vert\nabla f(\mathbf{x}_p{}^{(0)})\right\Vert}$	$2N_p+2N_p+2N_p$	$2N_p-1+2N_p-1$
$DFT\{m[\tau_l]\}$ to signal detector		$4N\log_2 N$	$4N\log_2 N$

Table 3.3 Complexity of operation in the adaptive Newton tracking

		Real Multiplications	Real Additions
Initial Stage	$Hessian(f(\mathbf{x}))$	$2\lvert\mathbf{\Theta}\rvert+1$	$2\lvert\mathbf{\Theta}\rvert-1+4N_p$
	$(\lambda\mathbf{I}_N+Hessian(f(\mathbf{x})))^{-1}\nabla f(\mathbf{x}^{(k)})$	$[\bullet]^{-1}_{mN_p}+2N_p(2\lvert\mathbf{\Theta}\rvert+1)$ $+(2N_p)^2$	$[\bullet]^{-1}_{aN_p}+4\lvert\mathbf{\Theta}\rvert+N_p(6\lvert\mathbf{\Theta}\rvert-1)+$ $(2N_p-1)(2N_p)$
	ex: $\lvert\mathbf{\Theta}\rvert=192, N_p=6$	5149+$[\bullet]^{-1}_{mN_p}$	8213+$[\bullet]^{-1}_{aN_p}$
Tracking Stage	Pilot direction	$4\lvert\mathbf{J}\rvert+4N_p\lvert\mathbf{J}\rvert+6N_p$	$2\lvert\mathbf{J}\rvert+2(2\lvert\mathbf{J}\rvert-1)N_p+4N_p-2$ $+2N_p$
	ex: $\lvert\mathbf{\Theta}\rvert=192,\lvert\mathbf{J}\rvert=8, N_p=6$	260	230
	Data direction	$2N_p(2\lvert\mathbf{\Theta}\rvert+1)+(2N_p)^2$	$4\lvert\mathbf{\Theta}\rvert+N_p(6\lvert\mathbf{\Theta}\rvert-1)+$ $(2N_p-1)(2N_p)+2N_p$
	ex: $\lvert\mathbf{\Theta}\rvert=192, N_p=6$	4764	7818
	$DFT\{m[\tau_l]\}$ to symbol detector (ex: N=256)	$4N\log_2 N$ (ex: 8192)	$4N\log_2 N$ (ex: 8192)

Table 3.4 Complexity of the adaptive Newton tracking

3.5 Mean Square Errors of Channel Estimators

Because the tracking parameters in adaptive Newton methods are path gains in the time domain, we concern the channel mean square errors (MSE) in it. MSE of the initial channel estimator is defined in the time domain as

$$MSE=E\{\sum_{\tau_l,\hat{\tau}_l}\left|\hat{h}[\hat{\tau}_l]-h[\tau_l]\right|^2\} \tag{3.24}$$

where $h[\tau_l]$ is the complex path gains with time delay τ_l and $\hat{h}[\tau_l]$ is the estimated path gain with estimated time delay $\hat{\tau}_l$. Note that the average time domain

channel power gain is equal to one, i.e. $E\{\sum_{\tau_l}|h[\tau_l]|^2\}=1$. In the computer simulations, time average of square errors is used to approach ensemble average as

$$MSE \cong \frac{1}{M}\sum_{m=0}^{M-1}[\sum_{\tau_l,\hat{\tau}_l}\left|\hat{h}[\hat{\tau}_l]-h[\tau_l]\right|^2] \tag{3.25}$$

where M is a large integer to satisfy the weak law of large numbers.

Because data decisions are done in the frequency domain, we concern the channel mean square errors (MSE) in it. Mean square errors of channels after Newton tracking is defined in the frequency domain as

$$MSE = E\{\frac{1}{N_{used}}\sum_{k=0}^{N_{used}-1}\left|\hat{H}_{g_k}-H_{g_k}\right|^2\} \tag{3.26}$$

where H_{g_k} is the frequency responses of the subcarrier with index g_k and $\hat{H}_{g_k}$ is the estimated frequency responses of the subcarrier with index g_k. N_{used} is the number of used subcarriers. Note that the average frequency channel power gain is equal to one, i.e. $E\{\frac{1}{N_{used}}\sum_{k=0}^{N_{used}-1}\left|H_{g_k}\right|^2\}=1$

In the computer simulations, time average of square errors is used to approach ensemble average as

$$MSE \cong \frac{1}{MN_{used}}\sum_{m=0}^{M-1}[\sum_{k=0}^{N_{used}}\left|\hat{H}_{g_k}-H_{g_k}\right|^2] \tag{3.27}$$

where M is a large integer to satisfy the weak law of large numbers.

In the latter simulation, $\mathrm{N_{used}}$ is 200 and $\mathrm{g_k}$ are the same as Table3.1 which is defined in IEEE 802.16 OFDM mode.

Chapter 4
Simulation Results and Discussions

Computer simulations are used to verify the mean square errors (MSE) of the initial channel estimator and MSE of the channels of the following OFDM symbols by adaptive Newton tracking. Besides, the bit error rate (BER) performances of the proposed methods with different parameters are also simulated. A two-path fading channel with relative path power profile {0, 0 (dB)} and a Universal Mobile Telecommunication System (UMTS) defined six-path fading channel with relative path power profile {-2.5,0,-12.8,-10,-25.2,-16 (dB)} are used in our simulations. The entire simulations are carried out in the equivalent baseband and the fading of the channel during one OFDM symbol is static. The preamble used in the initial channel estimator is defined in IEEE 802.16 OFDM mode and will be introduced in the section 4.1. The simulation results of the proposed initial channel estimator, followed by adaptive Newton methods will be showed and discussed in this chapter.

4.1 Introduction of a preamble define in IEEE 802.16 OFDM mode [20]

The downlink preamble defined in **IEEE802.16 OFDM mode** is as Fig. 4.1

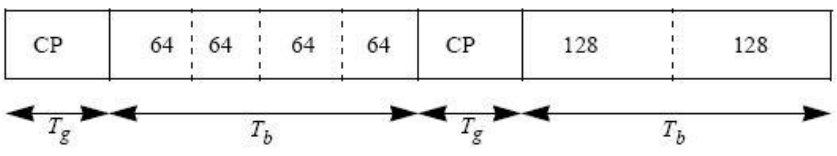

Figure 4.1 Downlink and network entry preamble structure

The frequency domain sequences for all full-bandwidth preambles are derived from the sequence:

P_{ALL}(-100:100) = {1-j, 1-j, -1-j, 1+j, 1-j, 1-j, -1+j, 1-j, 1-j, 1-j, 1+j, -1-j, 1+j, 1+j, -1-j,
1+j, -1-j, -1-j, 1-j, -1+j, 1-j, 1-j, -1-j, 1+j, 1-j, 1-j, -1+j, 1-j, 1-j, 1-j, 1+j, -1-j, 1+j, 1+j,
-1-j, 1+j, -1-j, -1-j, 1-j, -1+j, 1-j, 1-j, -1-j, 1+j, 1-j, 1-j, -1+j, 1-j, 1-j, 1-j, 1+j, -1-j, 1+j,
1+j, -1-j, 1+j, -1-j, -1-j, 1-j, -1+j, 1+j, 1+j, 1-j, -1+j, 1+j, 1+j, -1-j, 1+j, 1+j, 1+j, -1+j,
1-j, -1+j, -1+j, 1-j, -1+j, 1-j, 1-j,1+j, -1-j, -1-j, -1-j, -1+j, 1-j, -1-j, -1-j, 1+j, -1-j, -1-j,
-1-j, 1-j, -1+j, 1-j, 1-j, -1+j, 1-j, -1+j,-1+j, -1-j, 1+j, 0, -1-j, 1+j, -1+j, -1+j, -1-j, 1+j,
1+j, 1+j, -1-j, 1+j, 1-j, 1-j, 1-j, -1+j, -1+j, -1+j, -1+j, 1-j, -1-j, -1-j, -1+j, 1-j, 1+j, 1+j,
-1+j, 1-j, 1-j, 1-j, -1+j, 1-j, -1-j, -1-j, -1-j, 1+j,1+j, 1+j, 1+j, -1-j, -1+j, -1+j, 1+j, -1-j,
1-j, 1-j, 1+j, -1-j, -1-j, -1-j, 1+j, -1-j, -1+j, -1+j, -1+j, 1-j, 1-j, 1-j, 1-j, -1+j, 1+j, 1+j,
-1-j, 1+j, -1+j, -1+j, -1-j, 1+j, 1+j, 1+j, -1-j, 1+j, 1-j, 1-j, 1-j, -1+j, -1+j, -1+j, -1+j, 1-j,
-1-j, -1-j, 1-j, -1+j, -1-j, -1-j, 1-j, -1+j, -1+j, -1+j, 1-j, -1+j,1+j, 1+j, 1+j, -1-j, -1-j, -1-j,
-1-j, 1+j, 1-j, 1-j} (4.1)

The frequency domain sequence for the 4 times 64 sequence P_{4x64} is defined by:

$$P_{4x64}(k) = \begin{cases} \sqrt{2} \times \sqrt{2} \times conj(P_{ALL}(k)), k_{\mathrm{mod}\,4} = 0 \\ 0 \qquad\qquad\qquad\quad , k_{\mathrm{mod}\,4} \neq 0 \end{cases} \tag{4.2}$$

The frequency domain sequence for the 2 times 128 sequence P_{even} is defined by:

$$P_{even}(k) = \begin{cases} \sqrt{2} \times P_{ALL}(k), k_{\mathrm{mod}\,2} = 0 \\ 0 \qquad\qquad\quad , k_{\mathrm{mod}\,2} \neq 0 \end{cases} \tag{4.3}$$

In this channel estimator document, we take the 2 times 128 sequence P_{even} as our preamble, QPSK signals are transmitted, and the length of cyclic prefix (*CP*) is 64. In the following discussions, we refer the preamble defined in IEEE802.16 standard to the P_{even} sequence for brevity. The locations of data subcarriers and pilot subcarriers are showed in Fig. 4.2 and arranged in Table 4.1.

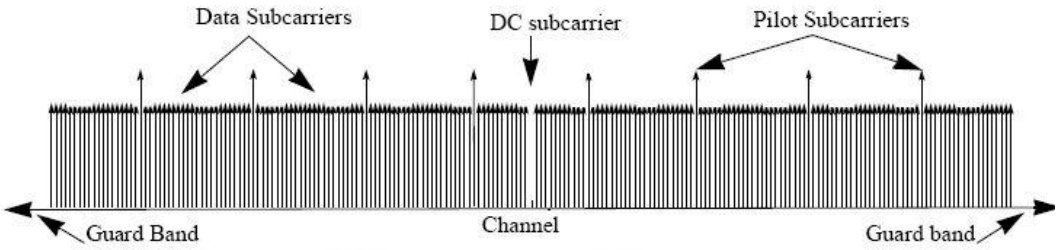

Figure 4.2 Frequency description of IEEE 802.16 OFDM mode

Frequency offset indices of guard subcarriers	-128,-127,…,-101 +101,+102,…,+127
Frequency offset indices of pilot subcarriers	-88,-63,-38,-13,13,38,63,88
Frequency offset indices of data subcarriers	-100,-99,…,-1,1,2,….,100 except the pilot subcarriers defined above

Table 4.1 Frequency description of IEEE 802.16 OFDM mode

According to this mode defined in the standard, the length of FFT is 256 but the number of used subcarriers is 200. Among the used subcarriers, 8 subcarriers are used for pilot tones, and the other 192 subcarriers are used to transmit information data.

Besides, the normalized cyclic-shift auto-correlation of the preamble defined in IEEE 802.16 OFDM mode is plotted as Fig. 4.2.

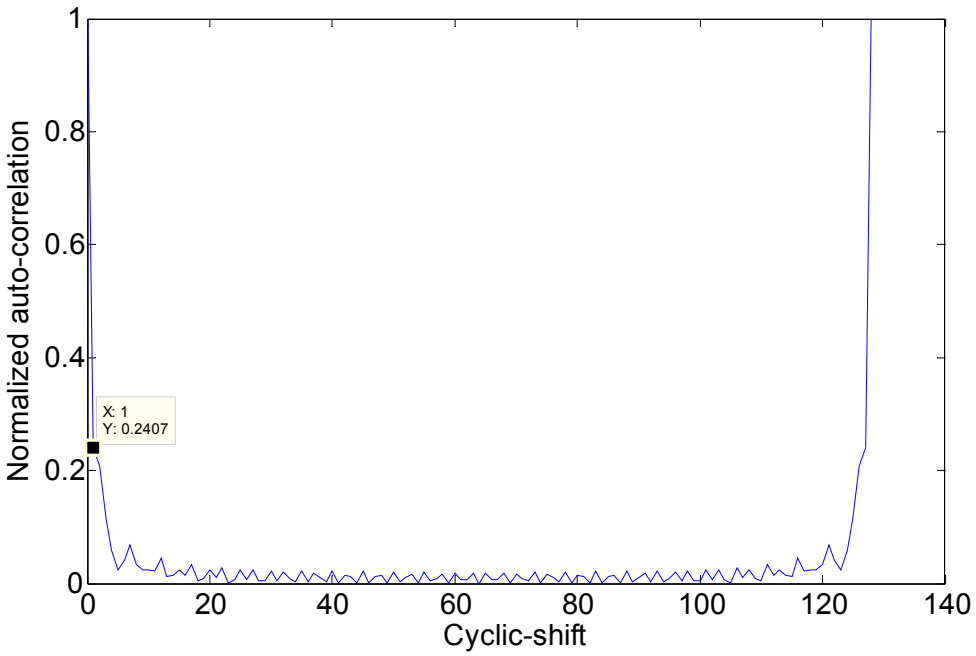

Figure 4.3 Normalized cyclic-shift autocorrelation function of the IEEE802.16 OFDM mode preamble

4.2 Initial Channel Estimators

In Fig. 4.1, the initial channel mean square errors (MSE) vs. delay spread of 3 estimators is showed. The MSE is defined in the time domain and the average channel power gain is normalized to one. The Multipath interference cancellation (MPIC) method is my proposed method. The inverse method is by multiplying the inverse of the preamble correlation matrix to the cross correlation between the received signals and the preamble which is introduced in 2.3.4. In the inverse discrete Fourier transform (IDFT) method, first, the channel responses of the known subcarriers at receiver end are estimated by LS solution. Second, the channel responses of the unknown subcarriers at receiver end are linear interpolated. Finally, interpolated channel responses are transformed by IDFT, and the largest N_p paths are selected to obtain the time domain channel response. Showed in Fig. 4.1, the

performance of the inverse method degrades with the increasing of the delay spread, which is mainly due to the increasing of the noise enhancement when the size of correlation matrix is large. Besides, the computing complexity increases severely with the size of the matrix due to the inverse function. The MSE of the IDFT method arises mainly from the mismatch of the interpolated channels. The variation of the frequency channel responses increases with the increasing of the delay spread, therefore, accurate interpolation of the channel responses for the guard band is difficult when the delay spread is large. The length of the observation window of $r_{yp}[\tau]$ is 118 in my proposed MIPC-based method. My proposal works well when the delay spread is large though having little degradation in small delay spread channels. The degradation arises mainly from the severe multipath interferences in which paths are close to one another.

4.3 Adaptive Newton Tracking

In Fig. 4.5, the mean square errors (MSE) vs. E_b / N_0 of my proposed initial channel estimator (phase I only and phase I followed by phase II which is called MPIC method for brevity) is showed. On the whole, the MSE of the MPIC method is smaller than that of the phase I only method especially in the high E_b / N_0 region. It illustrates that interference cancellation may have more effects when noises are small. The estimator path selection (N_p) mismatch somewhat degrades the performance. Besides, the degradation of the insufficient path selection case is more than that of the excess path selection case.

In Fig. 4.6, the bit error rate (BER) vs. pilot direction weighting α in the first Newton tracking iteration is showed. In general, the performances of the non-zero pilot weighting cases are better than that of the zero weighting case. In the two-path

channel model, the performances of the larger pilot weighting cases are slightly better because the pilot direction is more accurate than direction by decision data. In the later simulations, pilot weighting is chosen one.

In Fig. 4.7, the channel mean square error (MSE) after adaptive Newton tracking vs. E_b / N_0 is showed. In both the two-path and 6-path channel models, Newton tracking of 2 iterations reduces channel MSE significantly. It also demonstrates that Newton tracking converges fast. However, the channel MSE of iterations more than 2 fluctuates in the two-path model but only slightly in the 6-path model.

In Fig. 4.8, the bit error rate (BER) vs. E_b / N_0. BER with more than 2 iterations of Newton tracking is satisfying to approach the performance with perfect channel state information (CSI) assumption both in the two-path and 6-path model when the vehicle speed is 120km/hr.

In Fig. 4.9, the channel MSE after Newton tracking vs. E_b / N_0 with the path selection number N_p of the initial channel estimator as parameters is showed. When N_p is smaller than the path number of the true channel model, channel MSE degrades significantly. On the other hand, when N_p is larger than the path number of the true channel model, channel MSE degrades only slightly because redundant path parameters after Newton tracking may approach zero.

In Fig. 4.10, the BER vs. E_b / N_0 of the phase I only and MPIC initial channel estimator followed by adaptive Newton tracking in a 6-path channel model is showed. The performance of the MPIC method is better than that of the phase I only method in high E_b / N_0 regions because MPIC has more effects in those regions. Compared with Fig. 4.5, we know that Newton tracking has considerable tolerance about initial channel mismatch.

In Fig. 4.11 & Fig. 4.12, BER vs. E_b / N_0 with N_p as parameters are showed. In the 6-path fading channel, both in the vehicle speed 120km/hr and 240km/hr cases, there are less than 1 dB degradation when BER=10^{-3} is considered. The BER approaches that in perfect CSI assumption when N_p is selected larger than 6 and only 8 pilots used. However, in the two-path model, in the vehicle speed 240 km/hr case, there are about 7 dB degradation when BER=10^{-3} is considered. It may be because both pilots and decision data lose to track the channel variation accurately.

In Fig. 4.13, BER of the proposed method vs. packet length for vehicle speed= 120km/hr at E_b / N_0=30dB is showed. It shows that the BER performance still works well until packets with 500 OFDM symbols.

In Fig. 4.14, BER vs. E_b / N_0 for inter carrier interference (ICI) and ICI-free cases is showed. BER of both methods is based on MPIC-based initial channel estimator and adaptive Newton tracking. Different from the previous simulations, the channel responses in the ICI case is not static during one OFDM symbols. From the simulation, we known that ICI case has only little degradation compared with ICI-free case when the vehicle speed is 120km/hr in the 6-path fading channel.

In Fig. 4.15, BER vs. E_b / N_o of conventional decision directed methods is showed. Initial channel estimation is done by LS solution with the preamble. The channel responses of the unknown subcarriers are estimated by linear interpolation. The channel responses of the following OFDM symbols are estimated by decision directed method. After IDFT, the largest paths of the channel model are selected to suppress noise effects. Finally, DFT is used to obtain the frequency responses. Compared with the proposed adaptive Newton methods, DD methods have poor performances due to the variation between the channel responses of the successive OFDM symbols.

4.4 Simulation Environment

Simulation parameters are listed in Table 4.1 and briefly discussed in the following.

Carrier frequency	2GHz
Total bandwidth	5.12MHz
FFT size	256
Subcarrier used(N_{used})	200
Cyclic prefix	64
Modulation	QPSK
Pilot to data subcarriers ratio	3dB
Frequency offset indices of pilot subcarriers	-88,-63,-38,-13,13,38,63,88
Delay of multipaths (uniform distribution)	$0, 0.195, \cdots, 10.73\mu s$ $(0, 1, \cdots, 55$ sample period)
Vehicle speed(v)	120km/hr or 240km/hr

Table 4.1 Simulation parameters

From table 4.1, we can calculate some other important simulation parameters. Sampling time T_s is $\frac{1}{5.12MHz} = 0.2\mu s$, useful OFDM symbol duration T is $NT_s = \frac{256}{5.12MHz} = 50.0\mu s$, and complete OFDM symbol duration is $T + T_g = \frac{(256+64)}{5.12MHZ} = 62.5\mu s$.Take vehicle speed 120 km/hr for example, maximal Doppler frequency f_d is $f_c \times \frac{v}{c} = 2 \times 10^9 \times \frac{120 \times 10^3}{3600 \times 3 \times 10^8} = 222.2Hz$ and normalized Doppler frequency is $f_d \times (T + T_g) = 222.2 \times 62.5 \times 10^{-6} = 0.014$

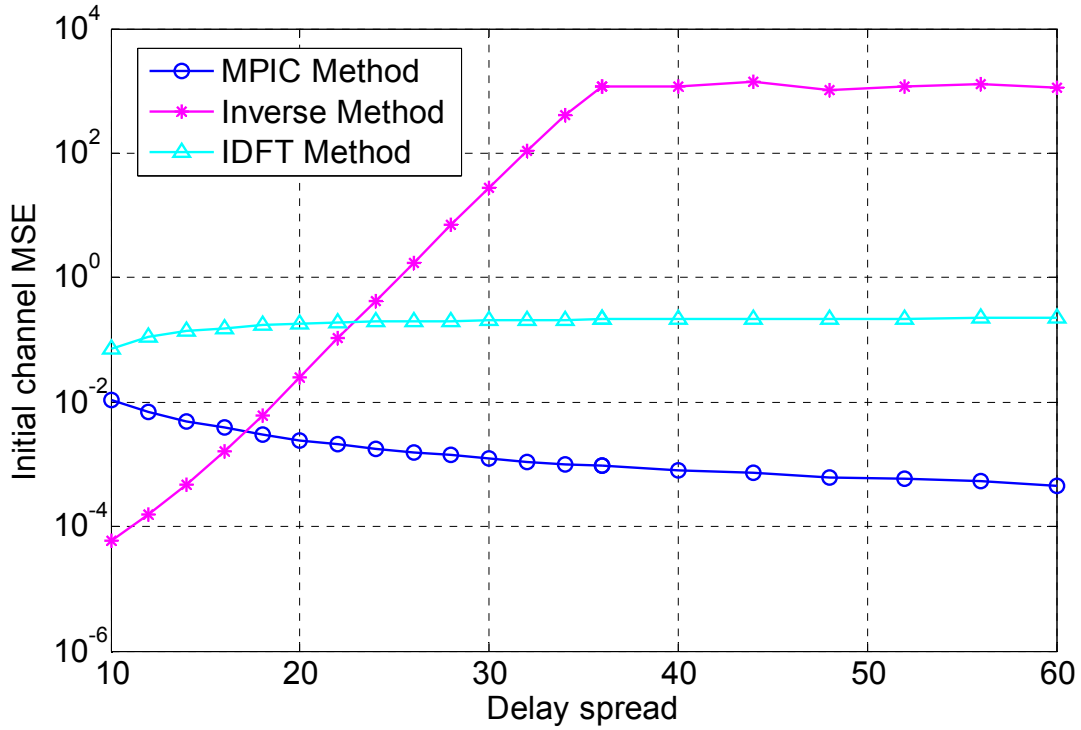

Figure 4.4 Initial channel MSE vs. delay spread of the inverse method, IDFT method and proposed MPIC method in a UMTS 6-path fading channel (v=120km/hr, E_b / N_o=30dB)

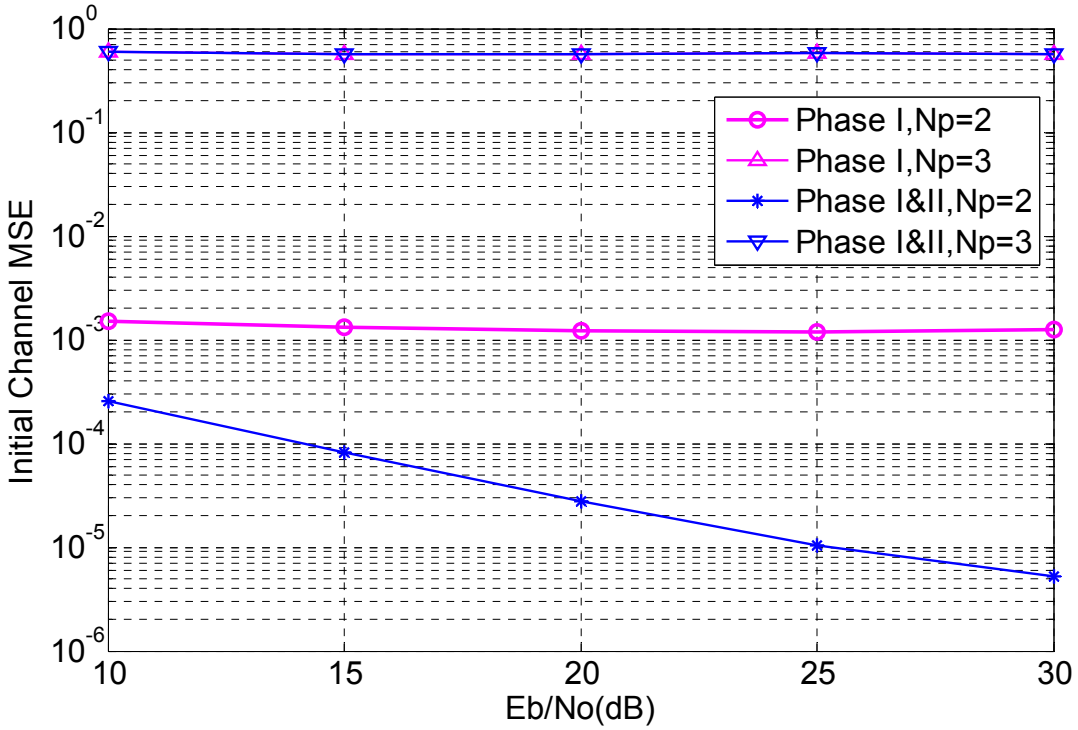

(a) In a two-path fading channel

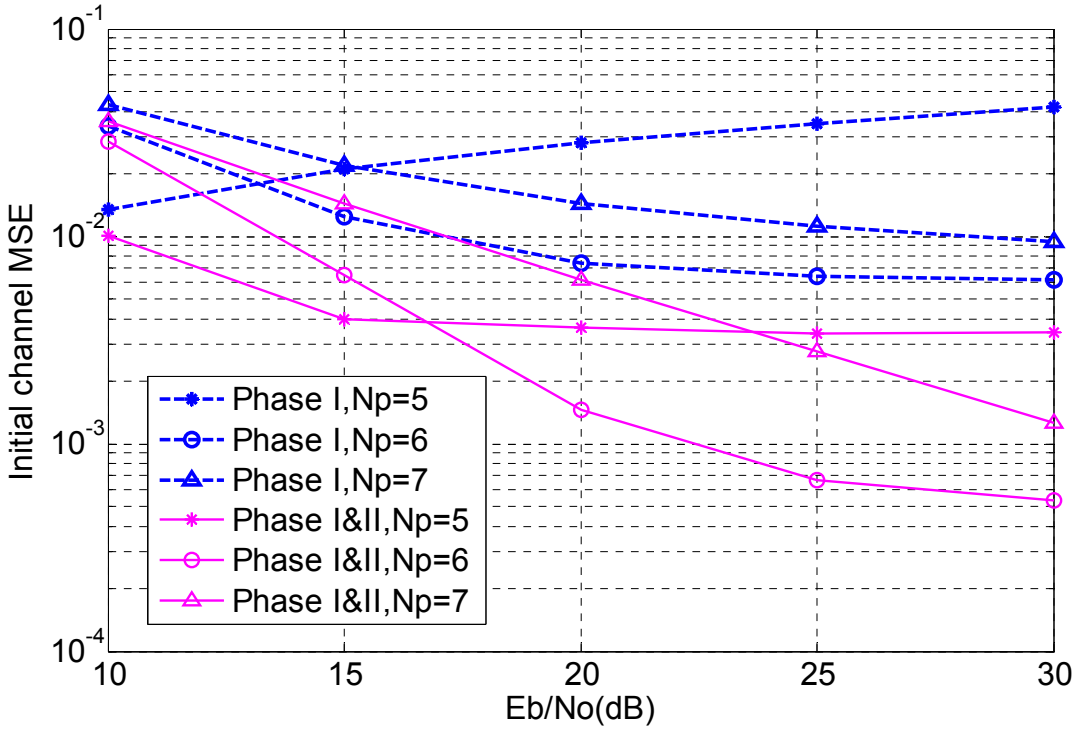

(b) In a UMTS 6-path fading channel

Figure 4.5 Initial channel MSE vs. E_b / N_o of the phase I only estimator and the phase I&II (phase I followed by phase II) estimator with N_p as parameters in (a) a two-path fading channel and (b)a UMTS 6-path fading channel (v=120km/hr)

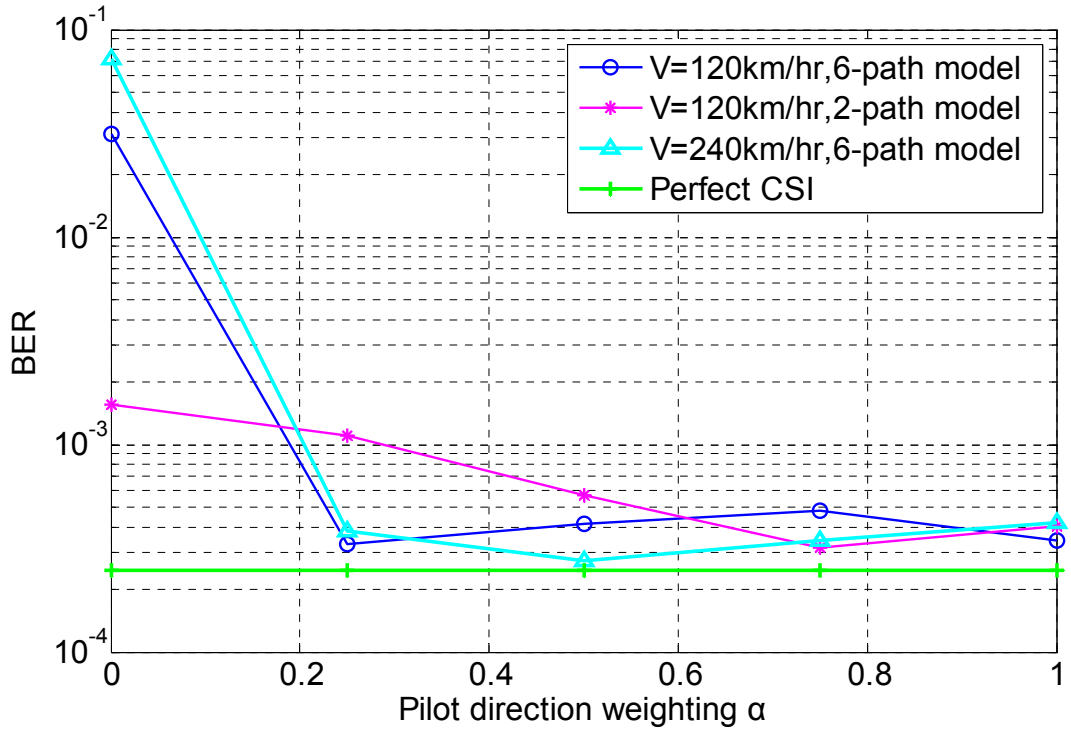

Figure 4.6BER of the Newton methods vs. pilot direction weighting α with vehicle speed v and channel model as parameters (E_b / N_o =30dB, packet length P=100, 8 pilots, β=2, Newton iteration number=5, and initial channel responses are estimated by the proposed MPIC method)

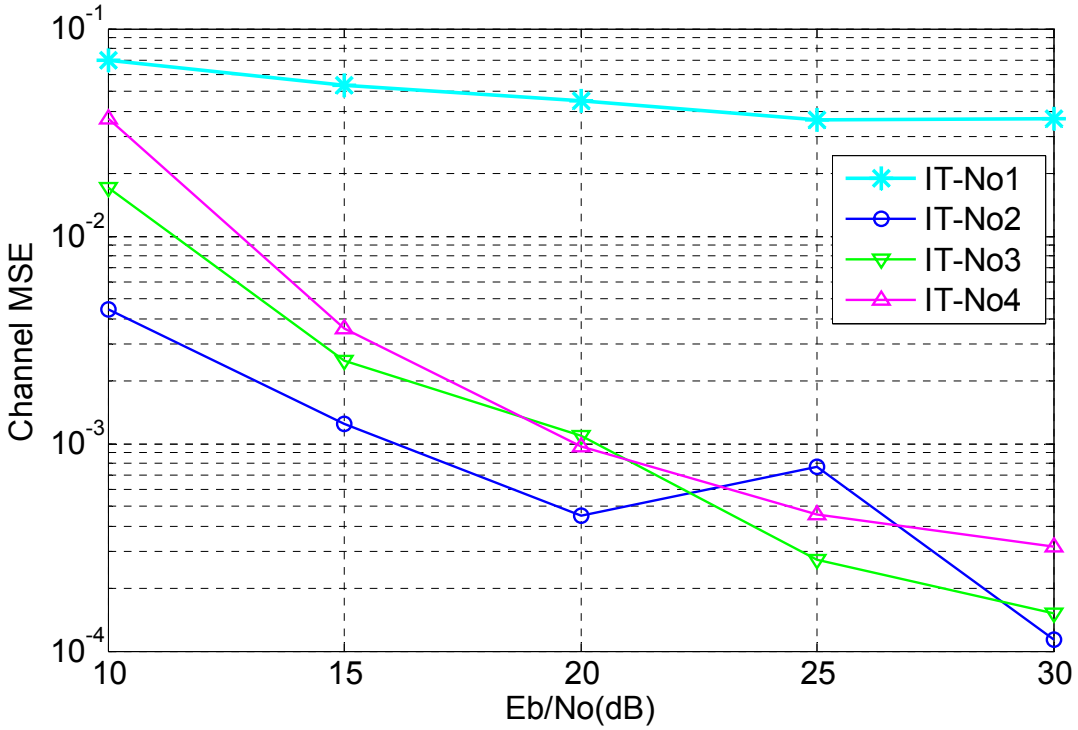

(a) In a two-path fading channel

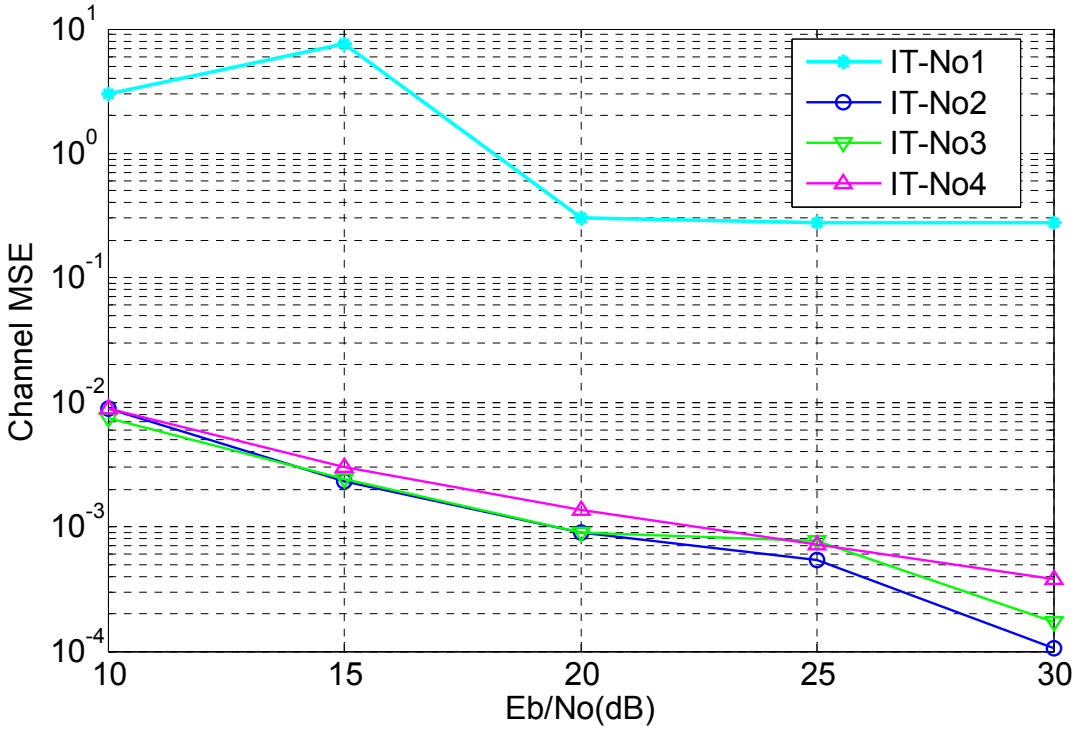

(b) In a UMTS 6-path fading channel

Figure 4.7 Channel MSE after Newton tracking vs. E_b / N_o with iteration number as parameters in (a) a two-path fading channel and (b) a UMTS 6-path fading channel(packet length P=100, 8 pilots, α =1, β=2, $N_p = 2$ in (a), $N_p = 6$ in (b), and initial channel responses are estimated by the MPIC method, v=120km/hr)

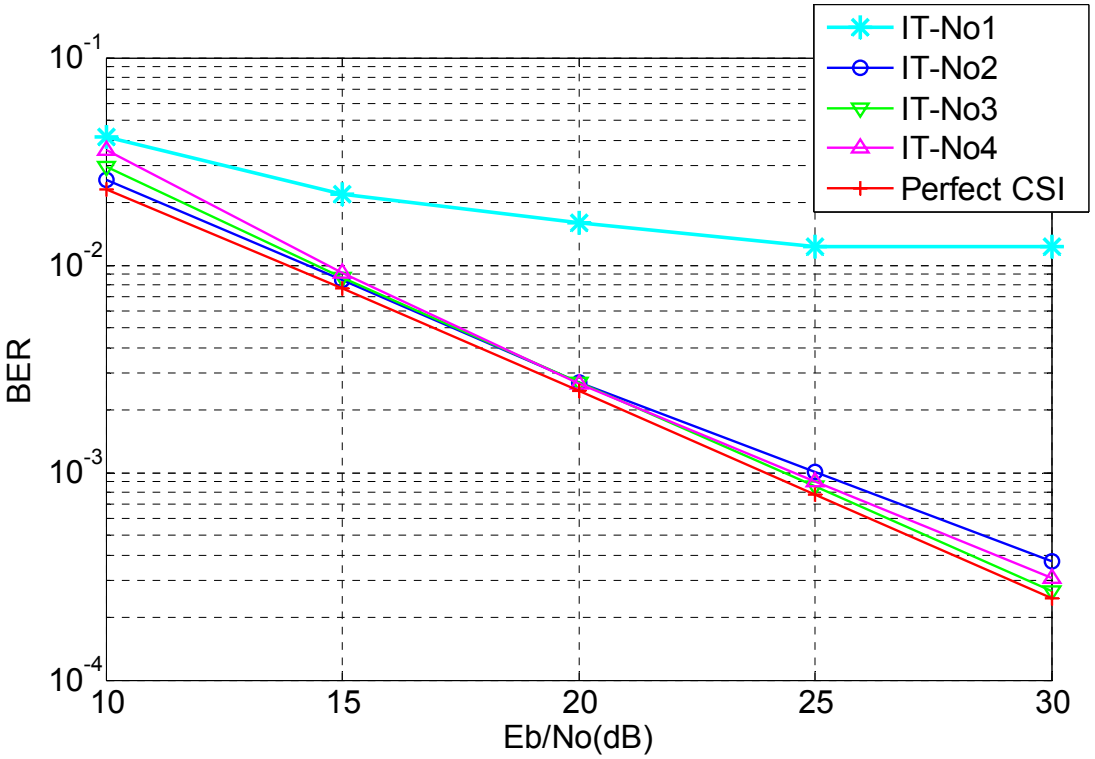

(a) In a two-path fading channel

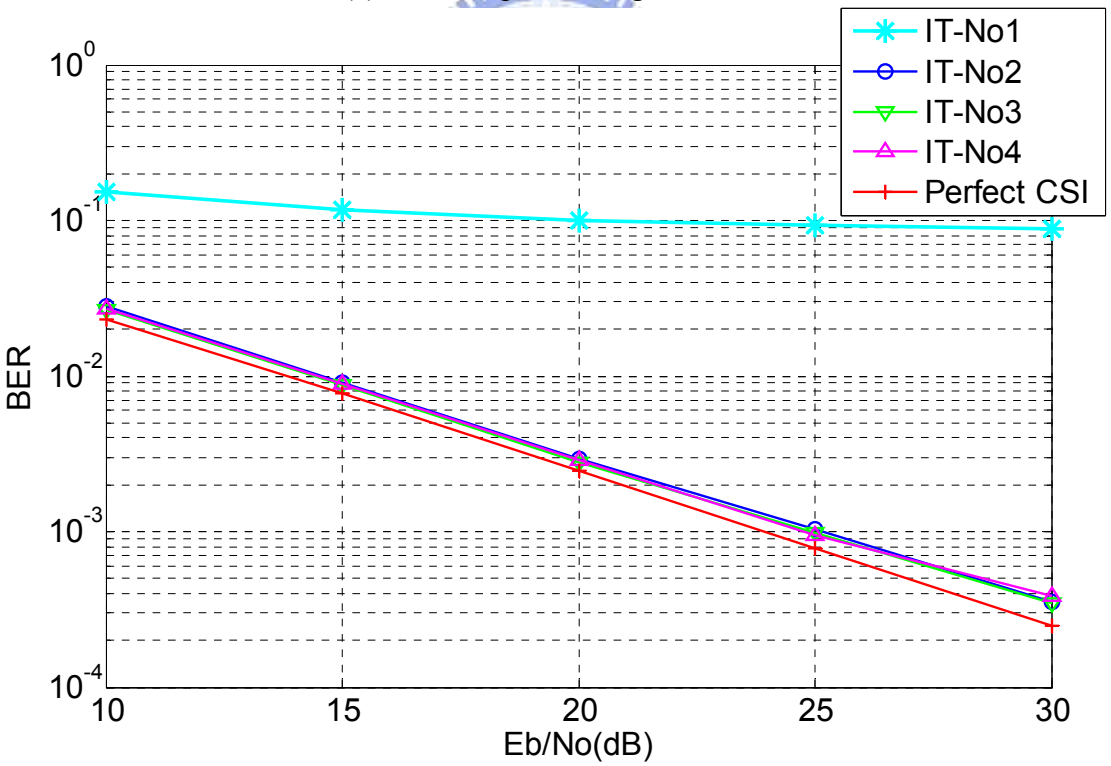

(b) In a UMTS 6-path fading channel

Figure 4.8 BER of the Newton methods vs. E_b / N_o with iteration number as parameters in (a) a two-path fading channel and (b) a UMTS 6-path fading channel(packet length P=100, 8 pilots, α=1, β=2, $N_p = 2$ in (a) and $N_p = 6$ in (b), and initial channel responses are estimated by the MPIC methods, v=120km/hr)

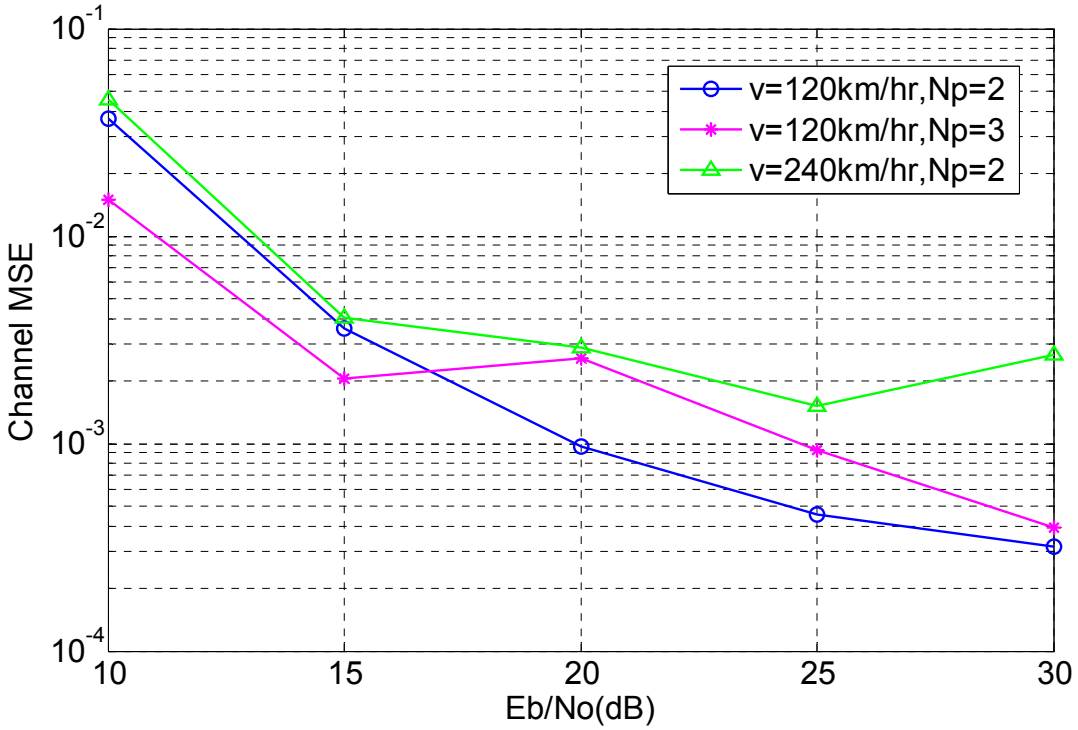

(a) In a two-path fading channel

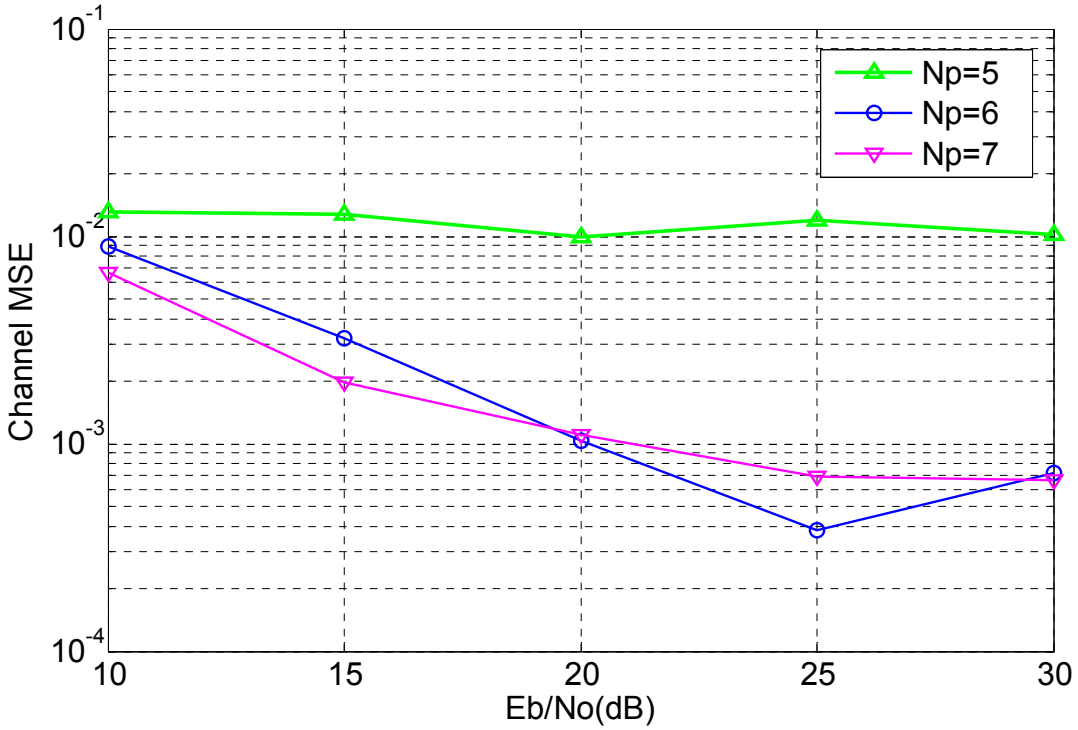

(b) In a UMTS 6-path fading channel

Figure 4.9 Channel MSE after Newton tracking vs. E_b / N_o with N_p as parameters in (a) a two-path fading channel, *v*=120km/hr or 240km/hr and (b) a UMTS 6-path fading channel, *v*=120km/hr(packet length *P*=100, 8 pilots, α=1, β=2,iteration number=5, and initial channel responses are estimated by the MPIC method

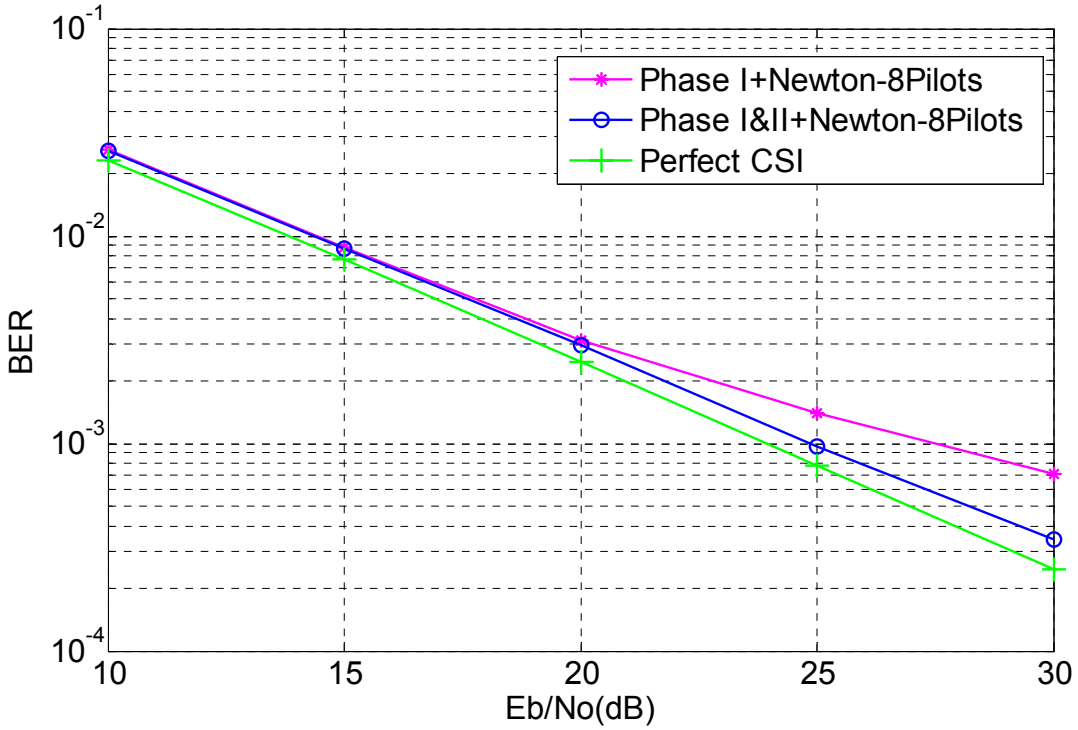

Figure 4.10 BER of the Newton methods vs. E_b / N_o of phase I only initial channel estimator and phase I&II (which is phase I followed by phase II) initial channel estimator in a UMTS 6-path fading channel (packet length P=100, 8 pilots, α =1, β=2, $N_p = 6$,Newton iteration number=5, v=120km/hr)

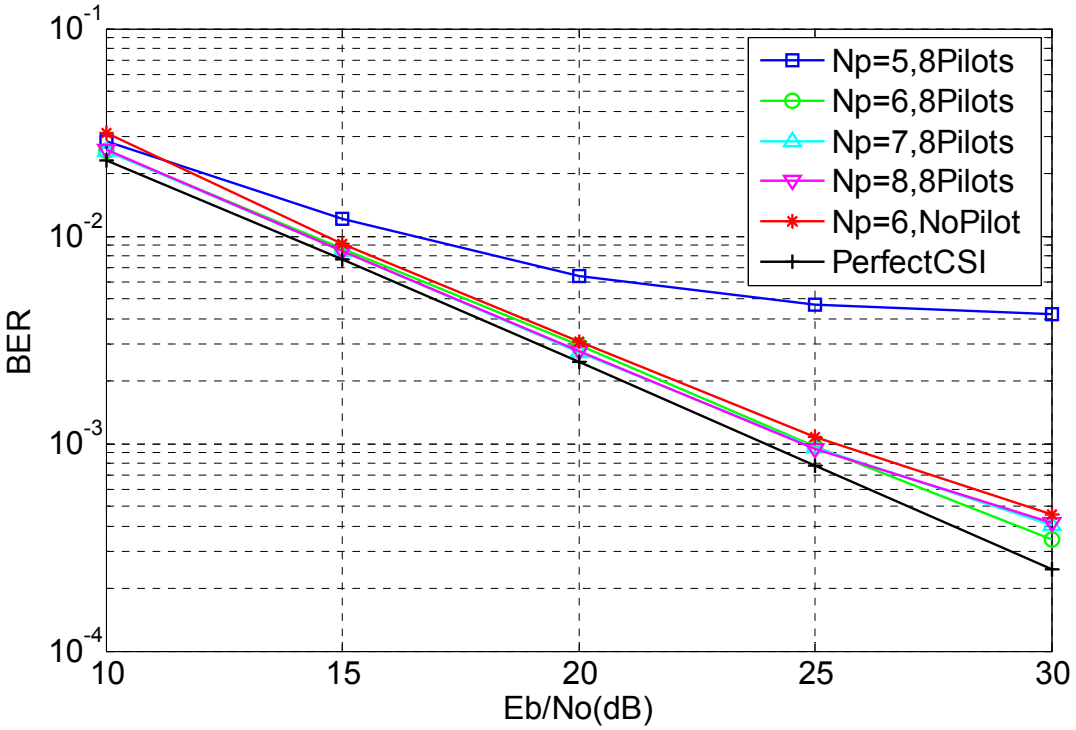

(a)Vehicle speed v =120km/hr

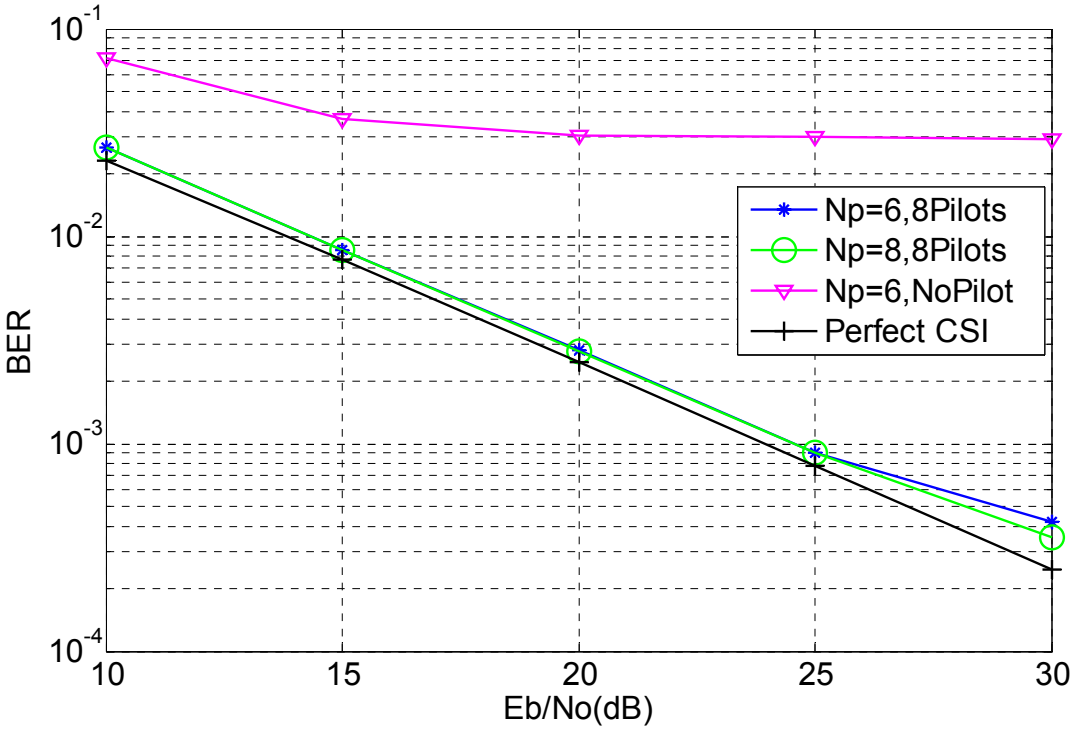

(b)Vehicle speed v =240km/hr

Figure 4.11 BER of the Newton methods vs. E_b / N_o in a UMTS 6-path fading channel with N_p as parameters in (a) v=120km/hr (b) v=240km/hr (Packet length P=100, 8 pilots or no pilot, α =1, β=2, Newton iteration number=5 and initial channel responses are estimated by the proposed MPIC method)

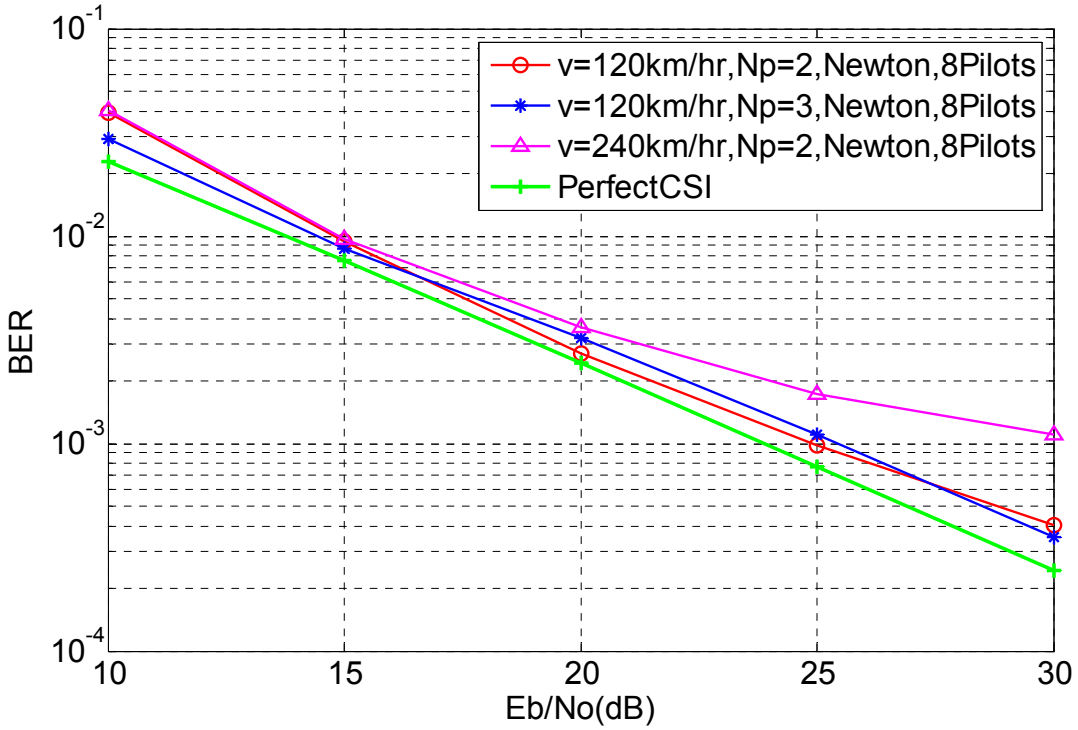

Figure 4.12 BER of the Newton methods vs. E_b / N_o in a two-path fading channel, with N_p and v as parameters (Packet length P=100, 8 pilots or no pilot, α=1, β=2, Newton iteration number=5 and initial channel responses are estimated by the proposed MPIC method)

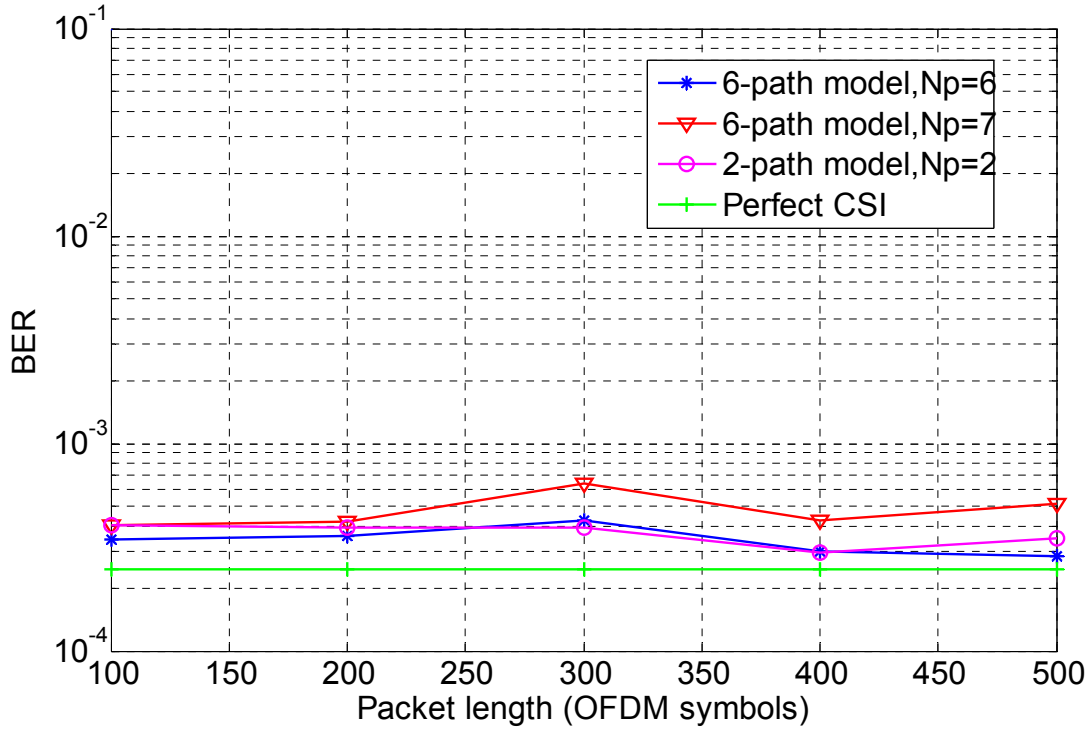

Figure 4.13 BER of the Newton methods vs. packet length for *v*=120km/hr in a two-path fading channel and a UMTS 6-path fading channel ($E_b / N_o = 30dB$, 8 pilots, α=1, β=2, Newton iteration number=5 and initial channel responses are estimated by the proposed MPIC method)

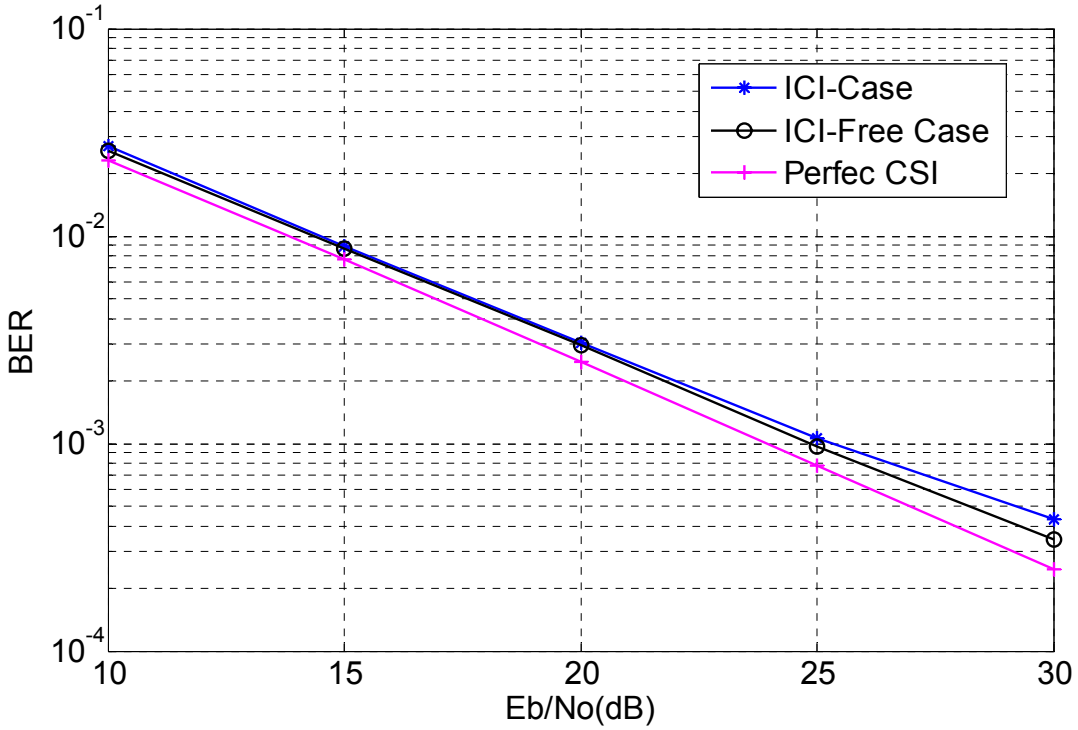

Figure 4.14 BER vs. E_b / N_o for ICI and ICI-free cases in a UMTS 6-path fading channel v=120km/hr (Packet length P=100, 8 pilots, α=1, β=2, N_p=6, Newton iteration number=5 and initial channel responses are estimated by the proposed MPIC method)

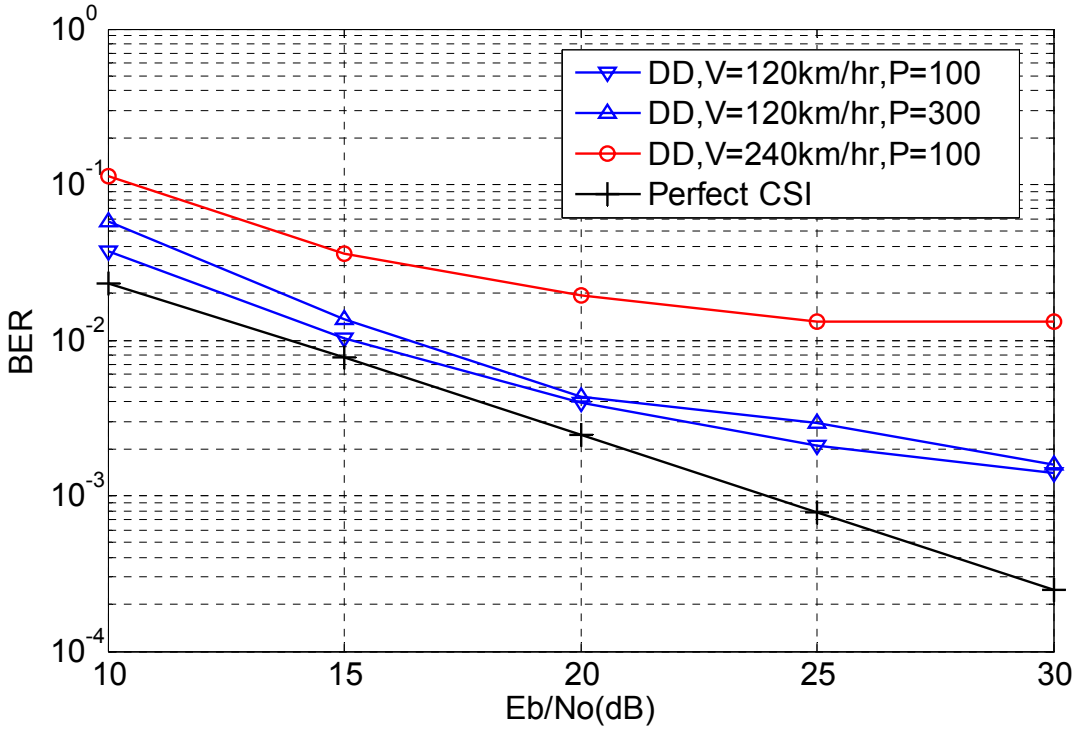

Figure 4.15 BER vs. E_b / N_o of conventional decision directed methods with vehicle speed and packet length as parameters (iteration number=2)

Chapter 5
Conclusions and Future Works

In this thesis, a semi-blind channel estimator is proposed. The semi-blind channel estimator consists of two parts: initial channel estimation method and channel tracker to track channel variations in the subsequent OFDM symbols. In the channel tracker, channel variation is tracked in the time domain. Therefore, channel mean square error (MSE) in the time domain is our main concerns in the initial channel estimator. The initial channel estimator is simulated with the preamble defined in IEEE 802.16 OFDM mode, and the adaptive Newton tracker is verified in high mobility channels (120 km/hr and 240 km/hr). From the simulation results, we know the proposed initial channel performs well in term of MSE in the time domain and the performance of the system after adaptive Newton tracking works well in terms of BER even in high mobility channels (120km/hr).

In conclusion, the proposed semi-blind channel estimator can achieve both bandwidth efficiency and estimation accuracy. Besides, there are no restrictions on the preamble in the initial channel estimator and no restrictions on the locations of the sparse pilots in the tracking stages, thus the proposed channel estimation methods also can be generally applied to OFDM systems.

There may be some skills to reduce computation complexity but not discussed in this thesis. Computation complexity reduction methods or DSP architectures could be investigated in hardware implementation in the future work.

Appendix

The pseudo code of Phase II algorithm in the initial channel estimator is as

- start from original $r_{yp}[\tau] = \sum_{n=0}^{n=255} y[n]^* p[(n-\tau)_{256}],\ \tau = 0,1,\cdots,L$
- initial:path_count=0
- for($l = 0, l \le \left[\frac{N_p}{2}\right], l++$)

{

$r'_{yp}[\tau] = r_{yp}[\tau] - \sum_{k=0,k\neq l}^{\left[\frac{N_p}{2}\right]} m[\tau_k] r([|\tau - \tau_l|]), \tau = 0,1,\cdots,L$ and $0<|\tau - \tau_l| < 128$

$\tau_l = \arg\max_{\tau}\{|r'_{yp}[\tau]|^2\}$

•while($\tau_l \ge$ the length of CP or $\tau_l = \tau_0, \cdots, \tau_{l-1}$)

{

$l = l+1;$

$r'_{yp}[\tau_l] = 0;$

$\tau_l = \arg\max_{\tau}\{|r'_{yp}[\tau]|^2\}$

}

$m[\tau_l] = r'_{yp}[\tau_l]$

if($l \le \left[\frac{N_p}{2}\right]$)

{path_count=path_count+1}

}

• for($l = \left[\frac{N_p}{2}\right] + 1, l < N_p, l++$)

{

$r_{yp}[\tau] = r'_{yp}[\tau]$

$r'_{yp}[\tau] = r_{yp}[\tau] - m[\tau_{l-1}] r[|\tau - \tau_{l-1}|], \tau = 0, 1, \cdots, L,$ and $0 < |\tau - \tau_{l-1}| < 128$

$\tau_l = \arg\max_{\tau} \{|r'_{yp}[\tau]|^2\}$

•while($\tau_l \geq$ the length of CP or $\tau_l = \tau_0, \cdots, \tau_{l-1}$)

{

$l = l + 1;$

$r'_{yp}[\tau_l] = 0;$

$\tau_l = \arg\max_{\tau} \{|r'_{yp}[\tau]|^2\}$

}

$m[\tau_l] = r'_{yp}[\tau_l]$

if($l < N_p$)

{path_count=path_count+1}

}

The pseudo code mainly consists of two loops. One is to estimate the larger $\left[\frac{N_p}{2}\right]$ paths and the other is to estimate the smaller $N_p - \left[\frac{N_p}{2}\right]$ paths. In the pseudo code, the goal of the while loop is to ensure the estimated path delay inside the guard length. If the estimated path delay is outside the guard length, it is considered an illegal path but the counting of the l loop is added one. The final legal path number is 'path_count' in the pseudo code. Therefore, the number of the legal paths may equal or less than the path number N_p in the estimator. After the phase II algorithm, 'path_count' in the pseudo codes will be the number of selected paths (instead of original N_p) to track channel responses in the adaptive Newton methods.

Bibliographies

[1] R.W Chang, “Synthesis of band-limited orthogonal signals for multichannel data transmission,” *Bell Systems Technical Journal*, Volume 46, December 1966 Page(s):1775-1796,

[2] Weinstein S. and Ebert P., “Data Transmission by Frequency-Division Multiplexing Using the Discrete Fourier Transform Communications,” *IEEE Transactions on [legacy, pre - 1988]*, Volume 19, Issue 5, Part 1, Oct 1971 Page(s):628 - 634

[3] Peled A. and Ruiz A., “Frequency domain data transmission using reduced computational complexity algorithms,” *Acoustics, Speech, and Signal Processing, IEEE International Conference on ICASSP '80*.Volume 5, Apr 1980 Page(s):964 - 967

[4] William Y. Zou, Yiyan Wu, “COFDM: AN OVERVIEW,” *IEEE Transactions on broadcasting*, Volume 41, No. 1, Page(s):1-8.

[5] J. G.. Proakis, “*Digital Communications*,” McGraw-Hill, Boston, 3ed.1995

[6] Theodore S. Rappaport, “*Wireless Communications, principles and practice,*” Prentice Hall, 2ed.1996

[7] W. C. Jakes, “*Microwave Mobile Communications,*” John Wiley & Sons, Inc., 1994.

[8] Y. Li, L. J. Cimini, Jr., and N. R. Sollenberger, “Robust channel estimation for OFDM systems with rapid dispersive fading channels,” *Communications, IEEE Transactions on*, Volume 46, Issue 7, July 1998 Page(s):902 – 915

[9] Edfors O., Sandell M., van de Beek J.-J., Wilson S.K. and Borjesson P.O., “OFDM channel estimation by singular value decomposition,” *Communications, IEEE Transactions on*, Volume 46, Issue 7, July 1998 Page(s):931 - 939

[10] Rahman Q.M. and Hefnawi M., “Channel estimation methods for MIMO-OFDM system: time domain versus frequency domain,” *Electrical and Computer Engineering, 2004. Canadian Conference on*, Volume 2, 2-5 May 2004

Page(s):689 - 692 Vol.2

[11] Y. Zhao and A. Huang, "A Novel Channel Estimation Method for OFDM Mobile Communication Systems Based on Pilot Signals and Transform-Domain Processing," *Vehicular Technology Conference*, *1997 IEEE 47th* Volume 3, 4-7 May 1997 Page(s):2089 - 2093 vol.3

[12] Fernandez-Getino Garcia M.J., Paez-Borrallo J.M. and Zazo, S., "DFT-based channel estimation in 2D-pilot-smbol-aided OFDM Wireless Systems," *Vehicular Technology Conference, 2001. VTC 2001 spring, IEEE VTS 53rd* Volume 2, 6-9 May 2001 Page(s):810 - 814 vol.2

[13] Morelli M. and Mengali U., "A comparison of pilot-aided channel estimation methods for OFDM systems," *Signal Processing, IEEE Transactions on* [see also *Acoustics, Speech, and Signal Processing, IEEE Transactions on*] Volume 49, Issue 12, Dec. 2001 Page(s):3065 – 3073

[14] Rinne J. and Renfors M., "Pilot spacing in orthogonal frequency division multiplexing systems on practical channels," *Consumer Electronics*, *IEEE Transactions on*, Volume 42, Issue 4, Nov. 1996 Page(s):959 – 962

[15] Ye Li, "Pilot-symbol-aided channel estimation for OFDM in wireless systems," *Vehicular Technology, IEEE Transactions on* ,Volume 49, Issue 4, July 2000 Page(s):1207 – 1215

[16] Frenger P. and Svensson A., "A decision directed coherent detector for OFDM," *Vehicular Technology Conference, 1996. Mobile Technology for the Human Race., IEEE 46th*, Volume 3, 28 April-1 May 1996 Page(s):1584 - 1588 vol.3

[17] Ye Li, Seshadri N., and Ariyavisitakul S., "Channel estimation for OFDM systems with transmitter diversity in mobile wireless channels," *Selected Areas in Communications, IEEE Journal on*, Volume 17, Issue 3, March 1999 Page(s):461 – 471

[18] Ho, K.Y. and Leung S.H., “A generalized semi-blind channel estimation for pilot-aided OFDM systems,” *Circuits and Systems, 2005. ISCAS 2005. IEEE International Symposium on*, 23-26 May 2005 Page(s):6086 - 6089 Vol. 6

[19] Muquet, B., de Courville M., and Duhamel P., “Subspace-based blind and semi-blind channel estimation for OFDM systems,” *Signal Processing, IEEE Transactions on* [see also *Acoustics, Speech, and Signal Processing, IEEE Transactions on*], Volume 50, Issue 7, July 2002 Page(s):1699 – 1712

[20] *IEEE Std. 802.16-2001* “EEE Standard for Local and Metropolitan area networks Part 16: Air Interface for Fixed Broadband Wireless Access Systems”